

Maintenance Offshore Wind

Luuk van Dun



Maintenance Offshore Wind

by

Luuk van Dun

to obtain the degree of Master of Science
at the Delft University of Technology,
to be defended publicly on Wednesday November 1, 2017 at 10:00 AM.

Student number: 1529188
Thesis committee: Dr. F. Sliggers, TU Delft
Ir. T. Vehmeijer, Huisman Equipment
Ir. P. van de Male, TU Delft

This thesis is confidential and cannot be made public until December 31, 2018.

An electronic version of this thesis is available at <http://repository.tudelft.nl/>.



Contents

1	Project Definition	1
1.1	Background	1
1.2	Problem Statement	2
1.3	Current Developments	3
1.3.1	Anson Crane	4
1.3.2	Lagerwey Crane	4
1.3.3	Liftra Crane	4
1.3.4	Gamesa Flexifit	5
1.3.5	Vestas Crane	5
1.3.6	Conclusion.	5
1.4	Project Description	5
1.5	Rapport Structure.	6
2	Wind Turbine Specification	7
2.1	Support Structure	7
2.2	Top structure	8
2.2.1	Gearbox	8
2.3	conclusion	9
3	Systems	11
3.1	Heave Compensation	11
3.2	Dynamic Positioning	11
3.3	Stabilizing Cranes, Gangways and Platforms	12
3.4	Conclusion	12
4	Concepts and Selection	13
4.1	Concepts	13
4.1.1	Climbing crane	13
4.1.2	Self-lifting crane with clamp	13
4.1.3	Base attached crane	14
4.1.4	Pulley lifting method.	14
4.2	Evaluating Concepts	14
4.3	Selected Concept	15
4.3.1	Step-by-Step solution description	15
4.3.2	Problem Identification.	19
4.4	Conclusion	19
5	Introduction Clamp and Tower	21
5.1	Preliminary Design of the Clamp	22
5.2	Clamp Forces and Reaction Forces	22
5.3	Safety Factors	24
5.4	Tower and Load Specifications	25
5.5	Variables of Interest	26
5.5.1	Elasticity.	26
5.5.2	Number of Pads	27
5.5.3	Width and Height	27
5.5.4	Diameter and Thickness of the Tower	27
5.6	Conclusion	27

6	Finite Element Model	29
6.1	Variables	29
6.1.1	Elasticity	29
6.1.2	Number of Pads	30
6.1.3	Width and Height	30
6.1.4	Diameter and Thickness	31
6.2	FEM pre-processing.	31
6.2.1	Geometry and Element type	31
6.2.2	Mesh.	32
6.2.3	Boundary Conditions and Loads.	33
6.3	FEM - solution	34
6.3.1	von Mises stress	34
6.3.2	Linear Buckling Analysis	35
7	Model Verification	37
7.1	Geometric and loading	37
7.1.1	Length tower section.	37
7.1.2	Loading assumptions	38
7.2	Stress	38
7.2.1	Linear stress analysis.	38
7.2.2	Hoop stress	38
7.3	Buckling Analysis	40
7.3.1	Eurocode Circumferential Buckling Pressure.	40
7.3.2	Results comparison Eurocode with ANSYS simulations	42
7.3.3	Convert uniform loading profile	43
7.4	Conclusions.	45
8	Results	47
8.1	Elasticity	47
8.2	Number of Pads.	49
8.2.1	Increase in number of pads for constant pad width	49
8.2.2	Increase in number of pads for constant gap width	50
8.3	Width and Height	51
8.3.1	Centred Load	51
8.3.2	Eccentricity	52
8.4	Tower Diameter and Thickness	54
8.5	Conclusions.	56
9	Conclusions and Recommendations	59
9.1	conclusions.	59
9.2	Recommendations	60
A	Turbine data	61
B	FEM introduction	63
B.1	Pre-processing	63
B.2	Solution.	64
B.3	Post-Processing.	64
C	Hoop stress comparison	65
D	Offshore Wind Turbine	67
E	Tables	69
E.1	Pad Height and Width.	69
E.2	Number of Pads.	73
E.3	Diameter and Thickness (D=3m)	75
E.4	Diameter and Thickness (D=4m)	76
E.5	Diameter and Thickness (D=5m)	77
E.6	Diameter and Thickness (D=6m)	78

F	Charts	79
G	REpower reference turbine	83
H	Eurocode correction for pipelength	85
	Bibliography	87

Project Definition

1.1. Background

The awareness of climate change is growing due to the increase in climate disasters caused by global warming. One of the main contributors to global warming is the release of carbon dioxide when burning fossil fuels. To reduce the effect of global warming, large industrial countries agreed to reduce the production of greenhouse gasses in the Kyoto protocol in 1997 [11]. It can be seen as a victory that the largest emitters of carbon dioxide, China, United States, the European Union, India and Russia all signed the protocol and thereby underlined the problem of global warming and their willingness to change that. As a result industrial countries invest more in renewable energy from wind, water and sun.

The wind market has been growing rapidly the last decades to meet the growing energy demand. China, the United States and Europe are increasing their investments in wind energy. China is leading the pack with over 168 GW of power installed and expecting to produce 200 GW by 2020. The installed capacity of the United States doubled in six years from 40 GW in 2011 to 82 GW in 2017. A similar pattern can be observed in Europe, where the installed power was 93 GW in 2011 and is currently over 153 GW¹.

Nowadays the majority of the wind energy is generated from onshore wind turbines. However, the investments in offshore wind energy are rising caused by the lack of available land and suitable wind conditions. Out on the ocean the lack of space is not an issue and the winds are stronger and more consistent. Looking at the installed offshore wind capacity over the years an exponential trend can be observed from the first installed turbines in 2000 up to now (see fig 1.1). The plans for the near future keep following this trend and as a consequence the energy generation from offshore wind will grow. Although offshore wind is promising, the costs are high. The foundation needs to be installed on the seabed and the structure has to bear higher loads. Furthermore does the remote location make installation and maintenance more difficult and therefore expensive. The growing potential of offshore wind is sparking innovation on all fields; turbine size increases and specific tools for installation and maintenance are developed. All with the simple goal of reducing the costs of offshore wind energy.

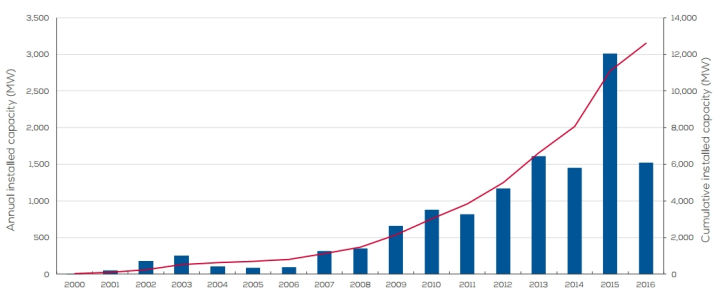


Figure 1.1: Overview of the total (red line) and annual installed capacity of offshore wind turbines. Source: windeurope

¹following data from the Global Wind Energy Council (GWEC)

1.2. Problem Statement

Operation and maintenance (O&M) activities of an offshore wind farm cover approximately one quarter of the total life cycle cost². This is considerably higher than for an onshore wind farm due to the harsh offshore environment. Offshore turbines need more maintenance but above all; specialized vessels and equipment are needed for service. As a result the downtime and the maintenance costs increase. Research from Faulstich et al. [8] shows that 95% of the turbine downtime is the result of failure of heavy components (such as bearings, blades, gearbox and generator). Knowing this two questions arise concerning the failure and the maintenance: (1) which main components fail and (2) how are these components currently replaced.

The extensive research of Carroll et al. (2016) [4], in which data of 350 offshore multiple MW offshore turbines was analyzed, gives a good insight in which components are most likely to fail. The yearly failure rate per component can be seen in figure 1.2. This yearly failure rate is a measure for how often a replacement or repair needs to be executed. For example; the yearly failure rate for a gearbox that needs major replacement is 0.154. This means that every 6.5 ($\approx 1/0.154$) years a major replacement has to be done for this component.

It can be observed that the gearbox and the generator need to be replaced relative often, with a yearly replacement rate of 0.154 and 0.095 respectively. These numbers are high, keeping in mind that replacement of heavy components is a time consuming and expensive procedure. An important conclusion from Carroll's research is that the failure of the generator and the gearbox are main contributors to high O&M costs. Improving this part of the maintenance cycle can help reducing the overall costs for O&M and hence reduce the costs for offshore wind power.

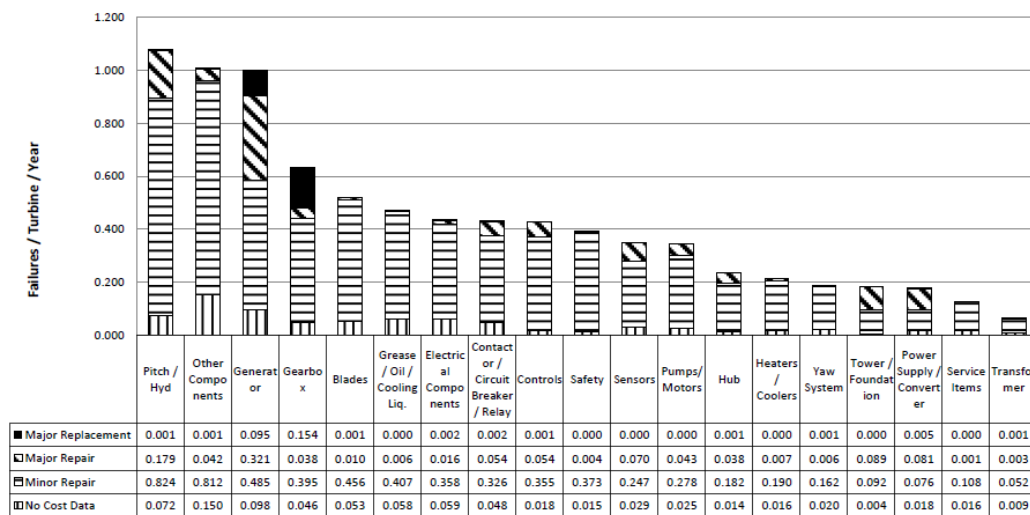


Figure 1.2: Component annual failure rate, source: Carroll et al. (2016) [4]

To get a better idea of the maintenance of an offshore wind turbine, this process will be described. Offshore turbines are equipped with a small service crane. Their load capacity varies, but they cannot lift more than 1-3 mt. Major components are defined as parts that cannot be replaced with the available service crane. For these heavy component replacements a crane vessel or jack-up is needed. In figure 1.3 a jack-up crane vessel is shown. It has four legs which can be lowered to the seabed and by doing so the vessel is lifted out of the water. In this lifted position the vessel motions are not influenced by wave and current forces and stability is assured. When the legs are installed, the crane can do its work; the top of the nacelle is opened, the crane takes the broken parts out of the nacelle and lowers them on the deck. The installation of the new parts is done by reversing this process.

²As stated by Garard Hassan in his investigation for the Crown Estate



Figure 1.3: Offshore wind turbine maintenance with a jack-up vessel

The advantage of this method is that all major components³ can be replaced. Even though the gearbox is the heaviest component, blade replacement is considered the most difficult operation. This because of the size of the blades can reach up to 88 meters⁴. Another advantage of this method is the stability, since the jacked-up configuration eliminates all ship motions. On the other hand also some disadvantages can be identified. The jack-up vessel needs to be equipped with a crane that can reach above the nacelle. In practice the cranes that are used are not designed for this purpose specifically. Standard cranes usually have sufficient lifting capacity but are unable to reach the height of the nacelle. Therefore large and too heavy cranes need to be used. Another weak point of this method is that a seabed investigation is required to avoid hazards like a punch through of the seabed or a leg that gets stuck in the mud. This can cause not only damage to the structure, but also hazardous situations for the crew⁵. The last downsides that need to be mentioned are the high costs of these operations and the long mobilization time of the vessels. The charging rates for jack up vessels or barges range from approximately 110.000 – 180.000 euro per day (following Dalgic et al) [6]. Even though these costs are very uncertain depending among others on the availability of certain vessels, the day rate of the equipment is a factor 10 larger than for onshore wind turbine maintenance.

In conclusion it can be said that replacement of major components of offshore wind turbines is a costly procedure and there is room for improvement. The components which need to be replaced most often are the gearbox and generator. Since a jack-up vessel is needed for this operation they are large contributors to high O&M costs. In the next section we will have a closer look at the developments in the field of major maintenance to get more insight in the problem.

1.3. Current Developments

The growth off the offshore wind industry is pushing innovation on all fields; turbines are getting larger and specific vessels and tools are developed to make the energy price of offshore wind more competitive. When looking specifically at major maintenance also a lot of developments can be seen. In this part the focus will be on these specific developments of major maintenance support systems.

³major component are defined as the parts which cannot be replaced with the service crane; gearbox, blades, hub, large bearings and the generator.

⁴LM wind produced the largest blade with a length of 88.4 m, used for the Adwen 8MW turbine

⁵<http://www.caithnesswindfarms.co.uk/fullaccidents.pdf>

1.3.1. Anson Crane

Anson is a Chinese company specialized in cranes. Currently they offer a self-climbing crane for major maintenance of wind turbines on land⁶. This solution (still in concept phase) can be described as follows: a crane is attached to the base of the wind turbine with a gripper. From there it climbs to the top of the tower using a hydraulic mechanism. By using this push-pull mechanism the crane can position itself at the top segment of the tower, from where the lifting will be conducted. The great advantage of this crane is that no adjustments on the tower are needed. A downside is that this solution is still in concept phase and that the focus here is on onshore purposes.

Development stage:	Concept phase
Installation of blade/gearbox:	Both possible
Usable on turbines of different dimensions:	Yes



Figure 1.4: Anson crane

1.3.2. Lagerwey Crane

Lagerwey, a Dutch company specialized in wind turbines, developed a method to install a turbine with a climbing crane⁷. The tower is installed piece-by-piece and the crane lifts itself by using a hydraulic arm which is attached to fixtures on the tower. An advantage of this solution is that a small crane can be used to install a complete wind turbine. A crucial downside is that it can only install wind turbines that are equipped with these fixtures. Therefore this method is only useful for installation (and maintenance) of in house developed turbine towers.

Development stage:	In production (proven concept)
Installation of blade/gearbox:	Both possible
Usable on turbines of different dimension:	No



Figure 1.5: Lagerwey crane

1.3.3. Liftra Crane

Liftra develops solutions for special lifting and transportation purposes and is specialized in products for the wind industry. They have developed a self-hoisting crane which can replace heavy components in the nacelle like the gearbox and generator⁸. The procedure is as follows: a cable is installed on top of the nacelle, the crane hoists itself from a container, climbs up the lifting wire and is installed on top of the nacelle from where the lifting can be done. This crane is already in use and Liftra is now focusing on further development of their system such that it can also be used for offshore purposes. A downside of this system is that it can only be used on specific turbines, or the nacelle needs to be adjusted such that this crane can be used.

Development stage:	In use
Installation of blade/gearbox:	Both possible, maximum lifting capacity of 32 tons
Usable on turbines of different dimensions:	Adjustments on nacelle necessary



Figure 1.6: Liftra crane

⁶<http://www.ansoncranes.com/wind-turbine-crane.html>

⁷<https://www.lagerweywind.nl/blog/2016/06/15/lagerwey-ontwerpt-s-werelds-eerste-klimmende-kraan/>

⁸Liftra leaflet and <http://liftra.com/product/shc/>

1.3.4. Gamesa Flexifit

Gamesa is one of the biggest producers of turbines and they have developed a maintenance crane which is installed on the nacelle⁹. This crane has to be installed by a crane and connects to the bottom of the nacelle as can be seen in figure 1.7. This system makes installation of the different components easier, but another crane is still needed to install the system on the nacelle. The system is already in use and can replace/install the drive train, generator, hub and blades. A downside is that the Flexifit can only be used on Gamesa turbines and has not been used in an offshore environment.

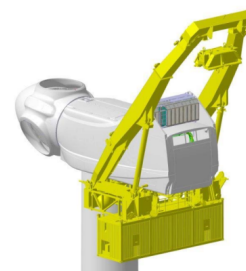


Figure 1.7: Gamesa Flexifit

Development stage:	In use
Installation of blade/gearbox:	Both possible
Usable on turbines of different dimensions:	No, only on Gamesa turbines.

1.3.5. Vestas Crane

Vestas is also developing a maintenance crane, which is still in conceptual phase¹⁰ and consist of a pulley system (which is used to install the maintenance system) and a crane. The installation of this system is done in three steps; (1) the service crane (that is situated in the nacelle) is lifting a pulley system to the nacelle and is installed on the nacelle. (2) The Vestas crane is equipped with a winch and lifts itself to the top of the tower. (3) The crane clings itself around the tower structure as can be seen in figure 1.8. From there all major components can be replaced using the rotating telescopic crane, including replacement of the blades. Vestas states that the crane will be able to lift weights up to 30 metric tons (mt). This will make their crane the first real alternative for replacing blades of a wind turbine and because it uses the tower structure, it is usable on turbines of different dimensions. The only downside is that development of the crane is still in conceptual phase.



Figure 1.8: Vestas crane

Development stage:	Concept phase
Installation of blade/gearbox:	Both possible
Usable on turbines of different dimension:	Yes

1.3.6. Conclusion

In conclusion it can be said that many maintenance systems are being developed or are already in use. Nevertheless three important downsides can be identified, namely: (1) the lifting capacity of the cranes is often not sufficient to replace the gearbox, the heaviest component of the vulnerable drivetrain. (2) The focus is mainly on onshore maintenance and (3) the Lagerwey, Gamesa and Liftra systems can only be used on specific turbines. However, Anson and Vestas use the tower structure for installing their maintenance system and therefore no adjustments are needed on the wind turbine.

1.4. Project Description

In the transition from a fossil fuel driven economy to renewable solutions, the activities in offshore wind energy are growing. Operation and maintenance costs of offshore wind turbines are high, therefore alternative methods should be developed to reduce these costs. The replacement of heavy components, like a gearbox or a generator, is a frequent occurring operation which could be improved. Therefore, in the first part of this research concepts will be generated which can replace the gearbox of an offshore wind turbine.

In the second part of this thesis the focus is on a promising concept: the self-lifting crane with clamp. This

⁹<http://w3.windfair.net/wind-energy/news/10101-product-pick-of-the-week-flexifit-from-gamesa>

¹⁰<http://kirt-thomsen.com/VESTAS-Towercrane>

concept consists of a small crane, which is attached to the tower structure by use of a clamping mechanism and is kept in position by generating frictional force. To generate this force, hydraulic cylinders are pressing the pads (contact surfaces of the clamp) against the tower structure. For the applicability of this concept it is of major importance that the structural integrity of the tower is maintained, while sufficient frictional force is generated to avoid the crane from slipping down during lifting operations. Therefore, in the second part of this thesis a feasibility study is done on the application of this clamping mechanism on wind turbine towers, where the contact surface of this clamping mechanism is subject of investigation.

1.5. Rapport Structure

In the first chapter the problem of high O&M costs was presented and current developments were investigated. This resulted in the project description where the main goal is twofold; (1) identify alternative lifting systems for offshore wind maintenance operations and (2) to perform a feasibility study on the application of the clamping system that is used to keep the maintenance system in position.

As a starting point the main subject of this investigation, the wind turbine tower, has to be defined. This is done in chapter 2, where the focus is on getting a better understanding of the wind turbine support structure, top structure and gearbox. This gives valuable insights in the structure and the load for which alternative maintenance systems have to be developed. Since the focus is on a maintenance systems for offshore application, also available techniques that are used in the offshore environment will be discussed in chapter 3. Those two chapters give a firm base to generate concepts.

In chapter 4 four concepts will be presented: the climbing crane, self-lifting crane with clamp, the pulley lifting method and the base attached crane. The first three concepts are installed on the top part of the wind turbine and operate from that position, where the base attached crane operates from the base of the tower. The working principle of these solutions is discussed and a selection is made. Finally the focus is on the most promising concept; the self-lifting crane with clamp. The process steps are described in detail and by doing so, a technical challenge for the application of this specific concept emerges; the crane is kept in position by frictional force. These high clamping forces are exerted on the thin shell structure of the wind turbine tower. For the concepts to work, the structural integrity of this tower should be investigated. This is used as input for the second part of the research.

The second goal of this thesis is to find a contact surface configuration such that the crane and its load is kept in position and the structural integrity of the tower is assured. To do so, the input for the research is defined in chapter 5: firstly a preliminary design of the clamp is given, the working principle of the clamp is described and the variables of interest are discussed. By use of finite element modeling the loading capacity of the tower structure is determined. In chapter 6 the variables of interest are translated into a model setup. Thereafter this model is verified in chapter 7. When the model verification has been done, the focus will be on the results of the FEM analysis for different configuration of the pad: elasticity of the contact layer, number of pads used, width and height of the pads. Furthermore, to assure this clamping mechanism works on towers of different dimensions (i.e. diameter and wall thickness combinations), the loading capacity is determined for a variety of tower dimensions. Finally conclusions and recommendations for future application are given in chapter 9.

2

Wind Turbine Specification

In the previous chapter the problem has been defined and an overview of the current developments is given. It became clear that (1) the lifting capacity of available systems is not sufficient and (2) that current systems are mainly focusing on onshore maintenance. Before starting the design of a system that can overcome these problems the offshore wind turbine and its component should be defined. Therefore in this chapter the support structure, nacelle and gearbox will be investigated. This gives insight in the structure for which a system has to be designed.

2.1. Support Structure

The wind turbine support structure consists of three parts, as can be seen in appendix D; (1) the tower foundation (mostly under water) (2) the transition piece, which connects the bottom with the top part and (3) the tower structure. The tower supports the rotor and the moving components, which are covered with the nacelle. The drive-train is mounted within which consist of a drive shaft, gearbox and generator. When designing a maintenance system the position and dimensions of these parts should be known.

First, the foundation is discussed. There are four types which are most commonly used: monopiles, tripods, jackets and gravity based structures (see appendix D). For maintenance purposes the ability to position close to the turbine tower is of great importance. The foundation footprint of a jack-up is larger than that of a monopile and because of the skirted foundation a safe positioning distance can be 10 till 15 meters from the tower.

On these foundations a transition piece is mounted, which ends above the waterline. Safe access points are also connected to this transition piece, like a boat landing, ladders and a platform for accessing the turbine. Above the transition piece, the access door of the turbine is situated in the bottom part of the tower. When accessing the turbine support structure this height is of major interest, therefore the variation in height of the transition piece above mean sea level (msl) has been investigated. Looking at a variety of wind farms in the North Sea the height varies from 3.5 meter (at Rodsand wind farm) to 23 meter (at Rhyl Flats wind farm)¹. The height of the transition piece depends on the weather and wave conditions on a certain location and therefore we see an increase of the transition piece on deeper locations.

The tower is the part of the turbine that connects the transition piece to the top structure. It transfers the load of the top structure and the environmental loads to the foundation. This tubular structure consists of steel plates which are rolled and welded together and is slightly tapered to reduce weight and costs of the structure. The tower dimensions are determined by the rotor diameter, wind conditions and clearance above the water level. Therefore the dimensions vary greatly as can be seen in the table 2.1. The dimensions vary, but a strong point should also be noted: almost all offshore wind turbine have this same tower structure that can handle heavy loads, which also can be used for maintenance systems as was seen in 1.3.

¹for more detailed information see table A.2 in appendix A

	Range	
Diameter top	2.3-4.2	m
Diameter bottom	4.2-6	m
Thickness	15-60	mm
Steel type	S355 -S235	-
Height hub	80-125	m

Table 2.1: Tower properties

2.2. Top structure

On top of the tower the moving components are mounted on a main frame (or bedplate). This frame is constructed such that it can carry the loads of the components and to transfer the thrust force exerted by the wind to the tower structure. The mainframe is made out of cast iron or a welded structure. It is this frame that can be particularly of interest for this research, since the mainframe is designed to handle heavy loads. For example; an favourable method to install the top structure is to lift it pre-assembled as a whole. When this is done the crane is connected to strong points on the top structure, where lifting eyes are attached for this purpose. These points on the structure are designed to handle the load of the top structure (with or without hub and blades) and therefore can also be of interest as loading points for a maintenance system. By analyzing top structure installation videos and pictures, the location of these connection points have been identified as can be seen in figure 2.1, the crane is attached to four lifting points on the mainframe, two in front and two behind the centre of gravity. The lines indicate the position of the lifting eyes and the indicated points are an example of the location where the lifting eyes are placed.

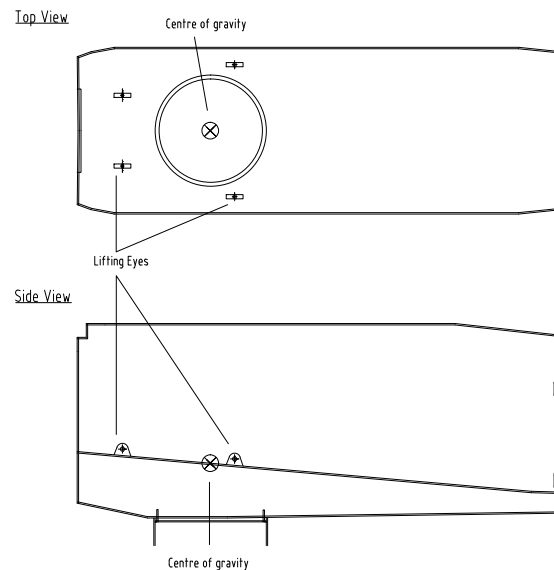


Figure 2.1: Schematic drawing of the top structure

2.2.1. Gearbox

The gearbox is selected as the replacement load. It is the heaviest component of the wind turbine power-train and its failure rate is high (as can be seen in fig 1.2). When this component can be replaced all other component of the drive-train can also be replaced because of their lower weight². The weight of the gearbox determines the lifting capacity of the system. When looking at gearboxes used in turbines there are many different setups. In general there are two types of stages that are used in gearboxes, namely planetary and parallel (helical) stages. The planetary stages are favorable for high torque and the advantage of parallel stages

²An exception has to be made for the rotor blades, because of their shape and size its replacement cannot be compared with replacement of a gearbox.

is its the stability at high speed operations. Planetary gears are lighter than parallel stages, but the increased complexity makes these stages more expensive. The mass of a gearbox will increase when the turbine power is increasing. Following Manwell et al. [10] the weight of a gearbox scales with the cube of the radius of a turbine. This is definitely the case when more stages or increasing ratios are used for larger turbines. However the developments in industry show otherwise; for multiple megawatt turbines (larger than 4 MW) the developers often choose for gearboxes with fewer stages connected to a medium speed generator and so reduce weight. In graph 2.2 the weight of the gearbox is plotted against the power of the turbine and here this trend is visible. The observation of this trend is of great importance when designing a system that should be scalable for turbines of other dimensions. In our case the focus will be on gearbox of a 5 MW turbine and based on the available data the system of development should be able to lift a gearbox of 50 mt. Because future developments show an increase in size, scalability of the concept is incorporated by also looking at turbines of other dimensions.

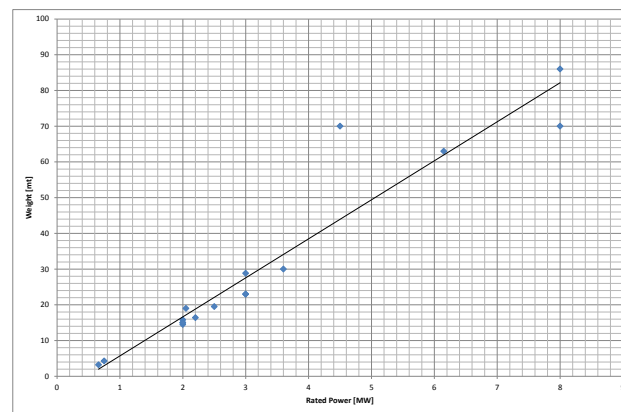


Figure 2.2: Gearbox weight graph of 17 turbines. For more data see appendix A

2.3. conclusion

In this chapter the offshore wind turbine and its components were looked at and several points have been defined that should be considered during the design of a maintenance system. Firstly; there is a great variation within wind turbine support structures. The type and configuration determine the accessibility of the structure. Nevertheless also a strong point is observed; almost all offshore wind turbines have a strong cylindrical tower which can be used for maintenance purposes. Furthermore the top of the nacelle is made to resist heavy loads and connection points were identified that could be used for maintenance purposes. Lastly, the focus was on the load, the gearbox. Here an important trend was observed (against expectations): gearbox weight increases linearly with the power of the turbine.

3

Systems

A major difference from the presented maintenance systems in section 1.3 is that in this research the focus is on wind turbines that are placed in an offshore environment, where the maintenance system and the components have to be transferred from a moving vessel to the wind turbine. In this chapter the focus is on available methods and systems that can be used for this purpose, such that the gap between the onshore operating systems and offshore operating systems can be filled.

3.1. Heave Compensation

There are two types of heave compensation systems, active and passive heave compensation. The difference between the two is that for active heave compensation a control mechanism systems which actively compensates for the motion using an external power source. A passive systems uses the energy from the motion to compensate for the motion and thereby reduces the effect of wave motion. The aim of actively heave compensation is to eliminate the effect of the heave motion such that the load does not move vertically as can be seen from the schematic overview in the figure below.

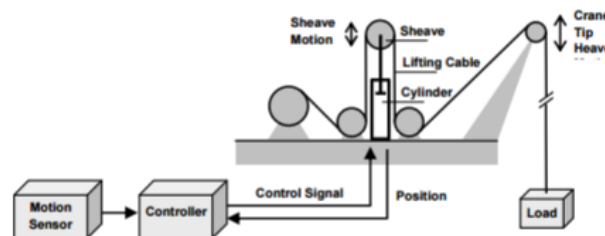


Figure 3.1: Heave compensation system

For this system a motion sensor registers the crane tip motion, which is used to control the hydraulic cylinder to actively compensate for the heave motion by extending or retraction of the piston. According to Salzmann [5] this system is accurate enough to compensate for 94% of a crane tip heave of 5m. Because hydraulic cylinders are used, this system is capable of heavy load lifting. IHC and Huisman Equipment develop this equipment. An alternative system with the same function is winch which is actively controlled and thereby compensates for the heave motion. For example ACE winches offers this type of equipment. A big advantage of heave compensation systems is that it is widely used in the offshore industry and the system is scalable and can be designed for heavy loads.

3.2. Dynamic Positioning

Vessels which are used for offshore purposes often need to operate in a specific position from which it cannot move during operation, such as drilling or lifting. Anchoring or lifting using a jack up is not always possible and therefore dynamic positioning is required to keep a vessel on a fixed position. Dynamic positioning is also

an active measure to maintain position. Surge, sway and yaw are measured and a control system translates this information to the required propulsion needed and activates the thrusters to keep in position. These systems are commonly used in offshore industry and can be very accurate (depending on the equipment used).

3.3. Stabilizing Cranes, Gangways and Platforms

In the offshore industry cargo and personnel has to be transferred from moving vessel to a fixed platform. For this purpose gangways and stabilizing cranes have been developed, which can also adjust for roll, pitch and heave motion. These systems are also active motion compensating systems, where a ship has 6 degrees of freedom, which can all be compensated. In figure 3.2 a schematic view is given of the Ampelmann gangway principle. Here a platform is kept stable on six hydraulic cylinders which compensate mainly for heave, roll and pitch motion. These motion compensated platform can also be used for cranes, like the Ampelmann E8000 (capable of lifting 8mt) or the Barge Master T40 (lift capacity of 15 mt). For heavier equipment Barge Master also developed a stabilized platform which is capable of carrying 160 mt.

Other systems have been developed which compensate less motions like the MacGregor crane which compensates only for the three rotating motions; roll, pitch and yaw. A big advantage of these systems is that not the whole weight of the load needs to be lifted vertically by the hydraulic cylinders, which make the system less complex. Also the Kenz gangway uses a simplified principle as can be seen in figure??. The two hydraulic cylinders can extend or contract and compensate for the roll motion of the ship. The rotation platform makes sure the ladder is pointing at the right direction and the distance is controlled by the telescopic ladder.

A great advantage of stabilizing systems is that with accuracy loads can be transferred from a moving vessel to a static structure. However a downside is that the loading capacity for current available systems is low. The barge master stabilized platform is capable of compensating a load of 160 mt, but this is only a platform and it cannot transfer this load to another entity.

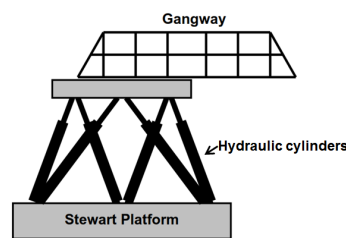


Figure 3.2: Schematic figure of ampelmann gangway system

3.4. Conclusion

In this chapter an overview has been given of positioning and stabilizing systems that can be used for developing a maintenance system. Heave compensation, dynamic positioning and stabilizing systems were discussed. Heave compensation systems show promising features, since these systems are sizable and already used in the offshore environment. Dynamic positioning is commonly used on vessels and therefore maintaining the position of a vessel is something that can be covered by using this technology. In the last section stabilizing equipment has been discussed and an important disadvantage has been identified: the currently available systems have a limited load capacity.

In the next chapter the information of the offshore wind turbine and available techniques will be translated into concepts.

4

Concepts and Selection

In this chapter concepts will be presented, evaluated and selected. Followed by a description of the working principle of the selected concept (installation, replacement and removal). Furthermore we will identify problems that need further investigation.

4.1. Concepts

In this chapter we will elaborate on the following four concepts; climbing crane, self-lifting crane, base attached tower and the pulley lifting method. To get a better understanding of the working principle of these concepts, we will look at two process steps: (1) installation/de-installation of the system, (2) replacement of a gearbox and. When the working principle is clear we shortly elaborate on the strong points and weaknesses of the concepts.

4.1.1. Climbing crane

working principle: this concept smartly uses the presence of the wind turbine tower and the main parts are the clamp/climbing system and the crane. From the deck of the ship this structure is placed above the transition piece of the wind turbine by using a crane. The climbing/clamping mechanism is locked around the tower and from this position the push-pull mechanism is activated to climb to the top of the tower structure.¹ In that position the crane is reaching above the nacelle and can remove the gearbox by simply lifting it out of the nacelle and lower it to the vessel. Guiding wires are needed to assure the load can be lowered safely to the the vessel. When the new gearbox is installed the installation process is reversed; the crane climbs down the turbine tower and a crane (motion compensated) lifts the system back onto the deck of the vessel.

Strong points and weaknesses: the strong points of this concept are; (1) no adjustments on the turbine are required, the system smartly uses the presence of the tower structure. (2) for this concept only a small crane is needed which doesn't needs the reach from the deck of the vessel to the top of the turbine. Also some weaknesses were identified; (1) the crane needs to be installed from a floating vessel onto the base of the tower. To do so, special equipment is needed. This can be a difficult task, because the height of the transition piece can be upto 23 m (as mentioned in section 2.1). Therefore the installation equipment needs to have a wide reach. (2) The tapered tower decreases in diameter from bottom to the top, the climbing crane should be able to deal with the decreasing diameter. (3) The gearbox needs to be lowered on the moving vessel. This is a delicate procedure, it should be done with precision and not damage the load. (4) To keep the system in position, high clamping forces are needed. Those forces should not damage the tower structure.

4.1.2. Self-lifting crane with clamp

working principle: This solution is quite similar to the previous solution, but has an important difference; the system is not climbing to the top of the structure, but is lifted to the top of the tower similar to the vestas

¹This pull pull principle can be simply explained as two rings which are alternately attached to the tower. When the top ring is clamped around the tower it 'pulls' the bottom part up. When the bottom ring is moved up, it clamps around the tower and the the top ring loosens its grip and 'pushes' itself itself up. By repeating this process the mechanism moves up the tower.

crane (see section 1.3.5). The installation goes in 3 steps: (1) a frame is installed on top of the nacelle by using the service crane. (2) This frame is used to lift the crane-clamp system from the vessel. (3) When the crane arrives at the top of the tower it clamps around the tower structure. For the removal and installation of the gearbox the same procedure is followed as for the climbing crane. The last step is to uninstall the system and here also an extra step is needed, namely the removal of the frame on top of the turbine, which is done using the service crane.

Strong points and weaknesses: a great advantage of this method is that, besides the system itself, no special equipment is needed. A deck crane or A-frame can be used to lift the system from the deck and normal winches can be used to lift the system to the top of the tower. Also here the absence of a large crane is a big advantage. The downsides of this method are: (1) the multiple step installation is time consuming; first the frame needs to be placed on top of the turbine and then the system can be installed. (2) Also here the lowering of the gearbox on the deck should be investigated and (3) the clamping force on the tower structure.

4.1.3. Base attached crane

working principle: the main component of this solution is a telescopic crane that is placed above the transition piece. Special equipment, like a deck crane is needed to bring the crane to the tower structure. There the system clamps around the bottom of the tower and the crane extends. In full extension the crane tip reaches above the nacelle. From there the gearbox can be lifted out of the nacelle and lowered to the deck of the vessel.

Strong points and weaknesses: by using the tower structure of the turbine, the lifting can be done from a static structure and no jack-up vessel is needed. Another advantage is that the crane can be attached to the tower at multiple locations, such that the loads are distributed over these segments of the tower structure. Also some difficulties should be addressed for this concept: the weight of the telescopic crane increases with its length and therefore the resulting crane will be a heavy structure. Installing this from a moving vessel onto the tower of the turbine is a challenging procedure, because reach and sufficient load capacity are required.

4.1.4. Pulley lifting method

working principle: this method uses a pulley that is installed on a frame on top of the nacelle. By using the service crane the pulley and frame are lifted (in parts if the lifting capacity is insufficient) to the top of the turbine and installed on the nacelle. When the pulley is installed the gearbox can be lifted from one side of the nacelle and lowered to the deck.

Strong points and weaknesses: a strong point of this solution is its simplicity; only a frame and a pulley are needed. Another advantage is that less steps are required for replacing a component, which reduces the operational time. Reducing complexity also has downsides: an investigation of the nacelle loading capacity must be done, to assure the connection points of the nacelle are strong enough to bear the loads. To make this concept work on different types of turbines, for every turbine another frame needs to be built.

4.2. Evaluating Concepts

In this section the four concepts will be compared and based on this comparison a selection will be made. There are different methods used for this purpose, of which the multi-criteria analysis is often applied. In this method the concepts are scored on different criteria, where the criteria have a weight, based on the importance of that specific criterion. Based on the scores on the different criteria, the concepts can be ranked. By using this quantitative method, it can be seen which concept scores highest and should be chosen. However an important downside of this method that should be addressed is that the results can be rather subjective, because it is hard to translate criteria weights in numbers. Therefore in this study has been chosen to do a qualitative comparison. The criteria on which the concept will be evaluated are (listed in order of importance); (1) technical feasibility, (2) safety, (3) company profile, (4) investment.

Technical feasibility can be interpreted as follows: till what extent are available techniques and equipment used for each concept. This is considered the most important criterion, because implementation of the method in the nearby future is valuable for the development of the offshore wind industry. When evaluating the concepts on technical feasibility, there was looked at; (1) the system that needs to be installed on the tower, (2) the process of installation of this system on the tower wind turbine tower and (3) on the (secondary) equipment needed to assist in the process of replacing a gearbox. The second criterion which will be looked at is safety; the offshore industry is characterized by the emphasis on safety and therefore is included in the assessment. With company profile the focus will be on how a concept fits with the activities of Huisman. The

last criterion is investment, where the costs of developing and production are evaluated.

Some strengths and weaknesses were already mentioned at the concept description. The concepts are given in order of desirable solution where the most desirable outcome is given first.

Self-lifting Crane - this concept has a big advantage above other concepts when focusing on technical feasibility; no other specialized crane is needed for the installation of the maintenance system on the tower structure. Also the system that needs to be installed on the tower structure is not complex, it consists of a clamping system and a crane.

Climbing crane – The most important difference with the self-lifting crane is that for installation of the climbing crane on the wind turbine tower specific equipment is needed. In section 3.3 it was shown that stabilized cranes are being developed. However the capacity and reach of these cranes needs to be extended to make this concept work and therefore implementation in the nearby future is not expected.

Base attached crane - This concept also has the problem of installation of the crane on the turbine tower. In this case the crane is even heavier and larger than the climbing crane and therefore the capacity of the equipment needed will also be a problem.

Pulley lifting method - This method is the least complex and uses available techniques and therefore the concept scores high on safety and investment. However, for this method a heavy lifting mechanism needs to be installed on the nacelle and it can only succeed when detailed information is available of the nacelle.

explanation and conclusion

The self-lifting crane is considered the most promising solution. The biggest advantages of this concept is that the system can be installed using available technologies and procedures. Here the use of winches make the concept score high on technical feasibility. Safety is criterion which is more difficult to measure, since the system still has to be designed and therefore can be designed such that safety is included. However the procedure can be judged on safety and on that point the climbing crane and base attached tower are considered more safe than the pulley lifting method and the self-lifting crane, because with the last two methods there are lifting wires involved and those systems are susceptible to swinging during installation, which can cause hazardous situations. When looking at company profile and investment the self-lifting crane is considered the best solution, because there are systems used which are familiar to the company like winches and a crane.

In conclusion can be said that the self-lifting crane is selected because of its technical advantages and because it fits the profile of the company. Its main technical advantage can be found in the installation of the system; there is no special equipment needed to install the system on the tower. Also the technology used for this system is available at Huisman equipment. Disadvantages should also be addressed: during operation, installation and de-installation heavy loads are lifted with wires and can cause hazardous situations when swinging. Another disadvantage is the multi-step installation procedure which is time-consuming. Nevertheless the self-lifting crane is considered to be the best solution for the installation of a gearbox. In the next part this solution will be described in more detail.

4.3. Selected Concept

4.3.1. Step-by-Step solution description

In this section a more detailed description of the selected solution is presented. This will be done by first looking at the different elements of the system and then the process of replacing a gearbox will be explained step-by-step.

Element description: in figure 4.1 an overview of the most important parts of the system is given: lifting frame, crane clamp system, A-frame, Rigging plate and winch:

Lifting frame: this is a light weight frame that is placed on the top of the Nacelle. The system of investigation differs from other tools on the market, because it needs to replace a gearbox, which is the heaviest part of the turbine that needs replacement. An implication of this requirement is that a system is needed which can bear this loads. This makes the crane clamp system quite heavy (in the range of 50mt). To lift this to the top of the tower, a strong structure is needed. Therefore a simple structure will be mounted to the lifting eyes of the Nacelle which have been identified in section 2.2. An sketch of the lifting frame is given in figure 4.2. This structure consists of several parts such that the lifting load of the available service crane is sufficient to install the frame. When installed on top of the nacelle, the lifting wires can be attached on the sheaves on both sides of the nacelle. In this configuration the load is equally distributed over both sides and so reducing the forces and moments on the lifting frame and on the nacelle structure.

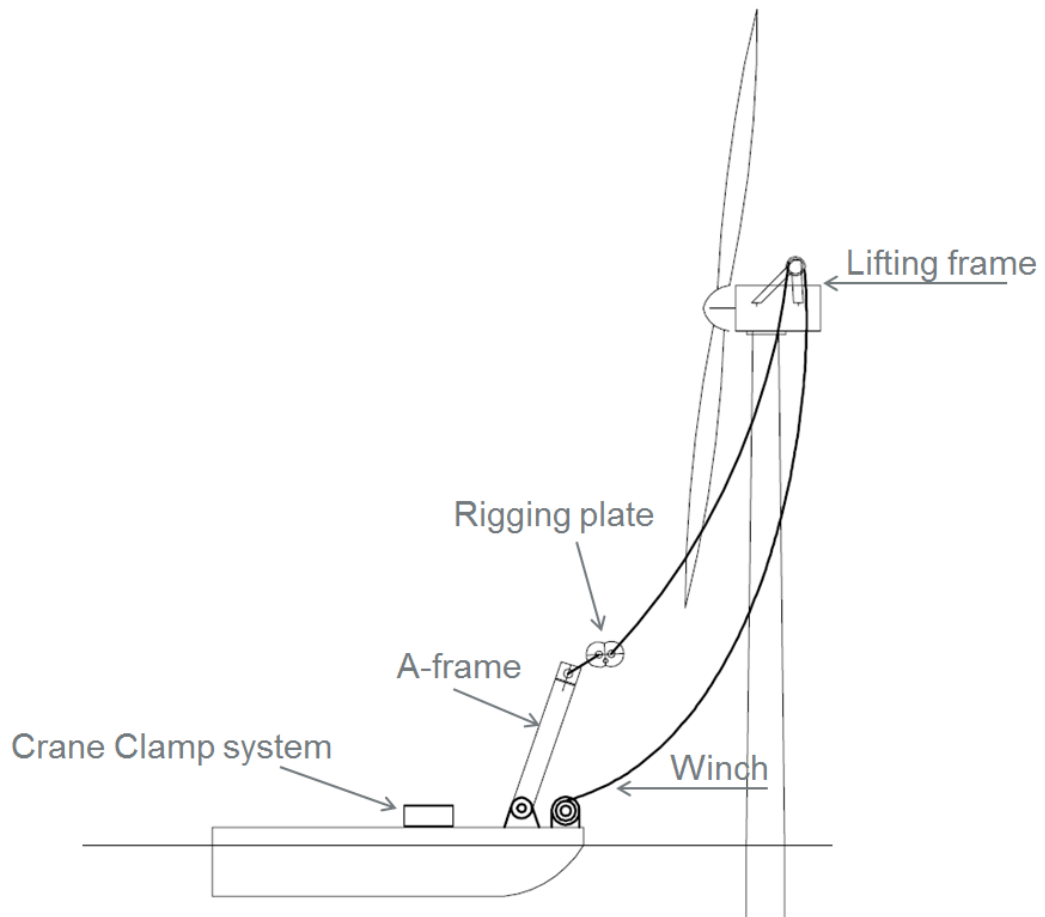


Figure 4.1: Overview system

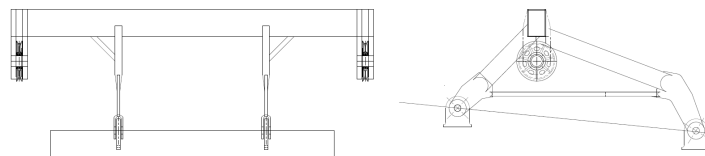


Figure 4.2: Top lifting frame, front view (left) and side view (right)

A-frame: the function of the A-frame is lifting the crane clamp system and later the gearbox from the deck. This type of lifting equipment is often used on vessel and can be considered as a simple solution for lifting loads from the deck. Also a deck crane could be used for this purpose.



Figure 4.3: Vessel equipped with A-frame

Crane clamp system: This is the most crucial part of the system, which consist of a crane, to lift the gearbox from the nacelle and install new part and a clamping system, that is needed to keep the system in

place on top of the tower. In figure 4.1 this is simplified as a rectangular box. In the next part this thesis we will have a closer look at this system.

Rigging plate: The rigging plate is a metal structure which connects the different systems together; load, lifting frame and the A-frame

Winch: The main function of the deck winch is to get the load to the top of the turbine. A heave compensation mechanism can be incorporated in the winch.

step-by-step solution description

Step 1: the top lifting frame is installed on top of the nacelle and the lifting wires are connected.

Step 2: the crane-clamp system is connected to the rigging plate and lifted from the deck of the vessel by the A-frame. At this point the load is completely carried by the A-frame.

Step 3: the load of the crane-clamp system is transferred from the A-frame to the deck winch.

Step 4: the crane-clamp system is moving to the tower of the turbine. In this position the A-frame wire is used as guiding wire, such that the movements of the system in the horizontal plane can be controlled. The clamp moves around the tower, such that the tower can be used to keep the system in the right position.

Step 5: the crane-clamp system is lifted to the top of the tower. Here the clamp locks itself around the tower and the crane is deployed. The clamp stays in place by friction with the tower surface.

Step 6: now the rigging plate is attached to the gearbox and the crane and can be lifted from the nacelle.

Step 7: the gearbox is lowered and the wire from the A-frame is used as a guiding wire, such that the gearbox can be lowered safely.

Step 8: when the gearbox is reaching the height of the vessel, the winch from the A-frame takes over; the gearbox is moving towards the A-frame.

Step 9: the gearbox reaches the A-frame and can now safely be lowered to the deck of the vessel.

Step 10: now the new gearbox can be lifted from the deck and the whole process is repeated in the reversed order.

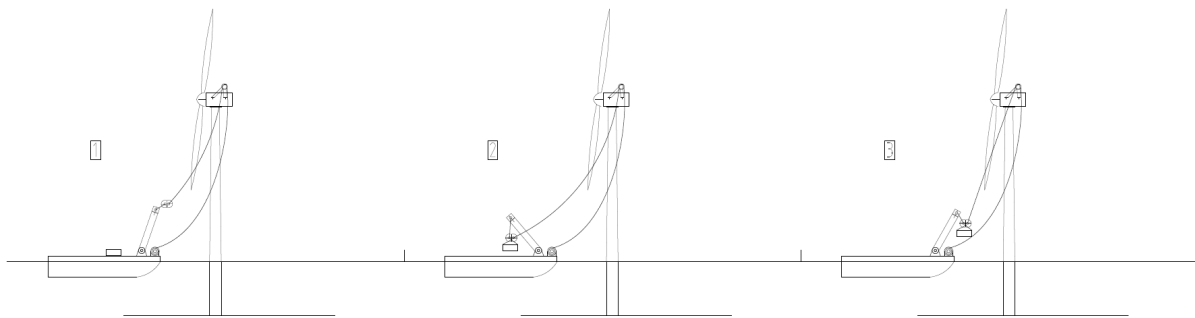


Figure 4.4: Step 1,2,3

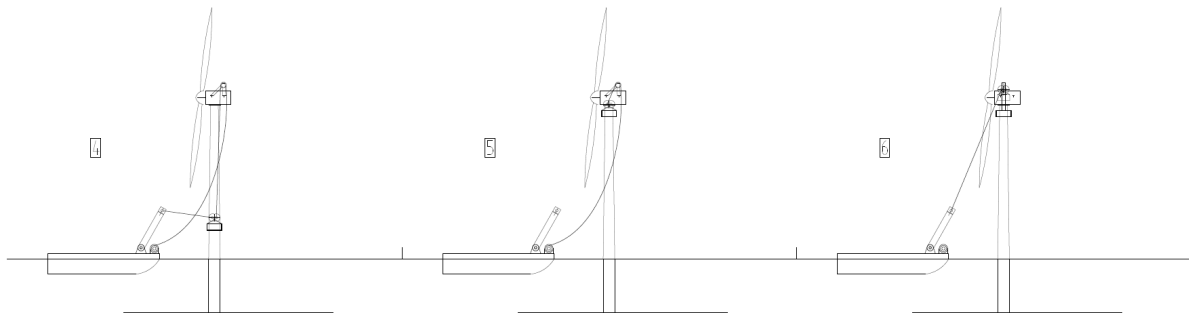


Figure 4.5: Step 4,5,6

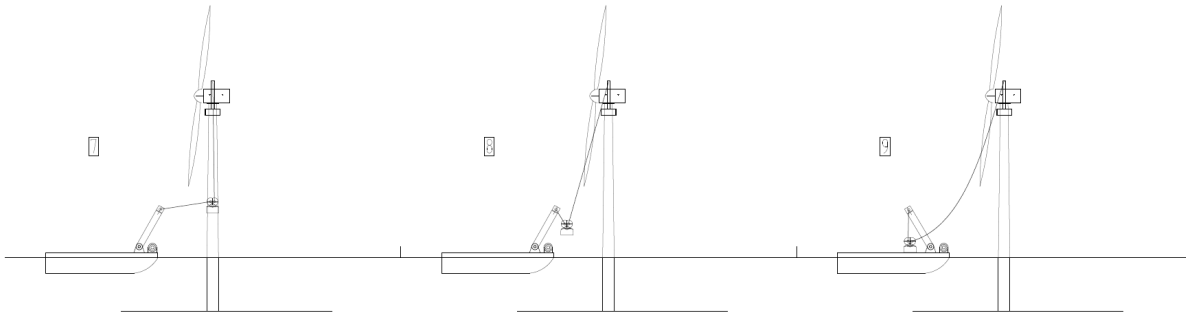


Figure 4.6: Step 7,8,9

4.3.2. Problem Identification

The step-by-step solution gives insight in the challenges that need further investigation. Two bottlenecks of the concept were identified:

Structural integrity of the tower: the clamp-crane system has to stay in place on the top of the wind turbine tower by friction, therefore the clamping force needs to be sufficient. With a load of fifty tons and the weight of the system the clamping forces are estimated on 10.000 kN^2 . This force is applied on a thin shell structure which has to resist these loads. The clamp has to be designed, such that the tower structure is not damaged when the clamping force is applied.

Deck lifting: in the chosen concept several loads need to be lifted from the deck of the vessel. The influence of the Movement from floating vessel to the tower structure.

4.4. Conclusion

Based on the current developments (section 1.3), wind turbine specifications (chapter 2) and available systems (chapter 3), we were able to present four promising solutions, namely; (1) the climbing crane, (2) the self-lifting crane with clamp, (3) the base attached tower and (4) the pulley lifting method. The working principle as well as the strong and weak points have been presented. Furthermore were these concepts judged on technical feasibility, safety, company profile and investment costs. Based on those criteria the self-lifting crane has been selected. Among other advantages, the technology used for this concept matches the company best. Subsequently, the installation, operation and de-installation procedure of this concept have been described and two problems have been identified, namely; (1) structural integrity of the tower and (2) lifting from the deck. The focus of this research will be primarily on the structural integrity of the tower, which will be done in the next part of the research.

²When looking at the reference 5MW turbine, the weight of the load (the gearbox) is 50mt. Besides the load also the weight of the system should be considered. Where the clamp has an estimated weight of 20 mt and the crane on 30mt. The crane weight is based on a SMST service crane with the required lifting capacity (30mt at 10m). The friction factor μ used is based on regular used friction factor 0.15 divided by a correction factor of 1.5, to adjust for non ideal conditions like a wet contact surface. Now for a centred load the clamping force can be determined as follows: $m_{total}g\mu = F_{clamp}$, where m_{total} is the total mass, g is the gravitational acceleration and F_{clamp} is the clamping force

5

Introduction Clamp and Tower

In the previous chapter the self-lifting crane has been identified as a promising concept. The clamp is placed on the wind turbine tower, a thin shell structure which should not be damaged when using the maintenance system. To be more specific; the stresses in the tower as a result of the clamping force should be lower than the yield stress and no buckling should occur when using the clamp. Therefore in this second part of the research the goal is to find a configuration of the tower contact surface that satisfies these requirements. This will be done following the flow diagram given in figure 5.1. But first a description of the complete process is given.

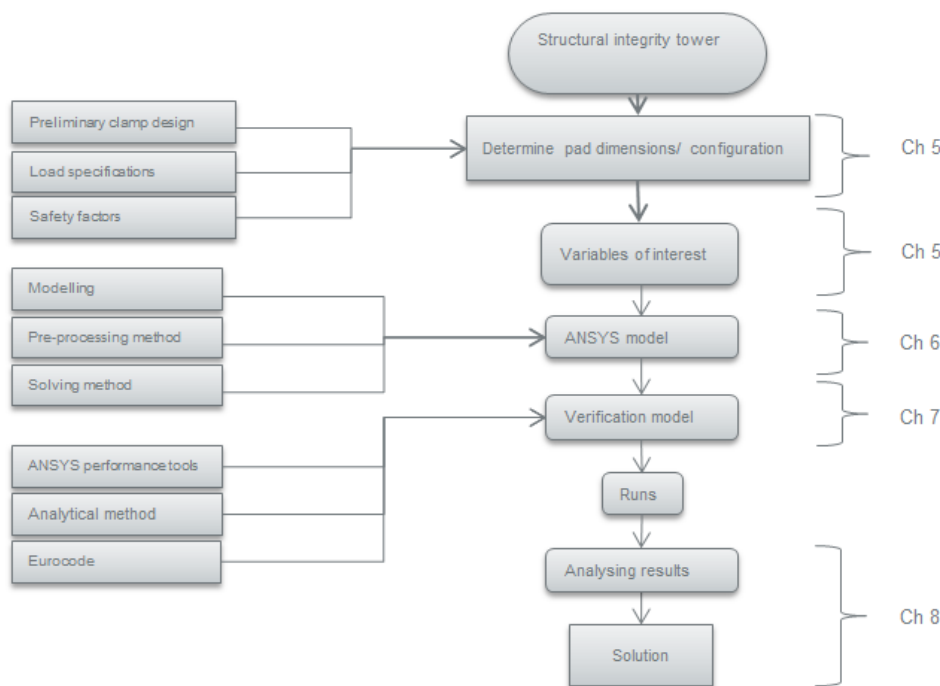


Figure 5.1: Flow model and chapters

The problem is used as the input for the diagram. Secondly, this problem is translated into a goal (or action): determine pad dimensions and configuration for which the tower structural integrity is assured. To reach this goal, the input has to be defined. This exists of a preliminary clamp design and working principle, determination of the loads and safety factors. Based on this input the research is designed. The next step is to define the variables of interest, which are: (1) elasticity of the contact material, (2) number of pads, (3) width, (4) height of the pad and (5) the tower dimensions (diameter and thickness).

Afterwards the variables are linked to a research method and molded into a research setup. In this thesis finite element modelling (FEM) is done with the software package ANSYS workbench 17.2. In this step the

variables are translated into a model that suits the FEM software and also the two failure criteria that will be checked are defined: (1) Von Mises stress and (2) linear buckling load.

The following step is verifying the constructed model. This is done using ANSYS performance tools and by comparing the results with literature. The loading assumptions are checked using the performance tools, followed by comparing the stress results with analytically determined results. The linear buckling analysis will be checked by comparing with European standards (NEN-en-1993-1-6 (2007): strength and stability of shell structures) [1].

When the model is verified it can be used to generate results, which is the next step of the process. These results are interpreted and analyzed. Here the maximum loading conditions will be given for the different pad configurations. Thereafter the solution is presented. The loading capacity for this presented solution is based on fixed tower dimensions (diameter is four meters and thickness is five millimetres). Now for this specific pad configuration the influence on the loading capacity is checked when the diameter and thickness of the tower is varied. By doing so it can be seen what the influence is of the loading capacity for variable tower dimensions. The results will be discussed in chapter 8. In this chapter the focus lays on defining the input; the clamp, loads and safety factors and the variables of interest.

5.1. Preliminary Design of the Clamp

In this part the basic principle of the clamp are explained and an elementary solution is given. In figure 5.2 a side view and a top view of the clamp can be seen. In the right figure, the clamp is sketched in an open and closed configuration. The red arrows indicate the movement of the frame when the clamp is opened. The reversed motion will be enacted when the system is lifted in position and the clamp is closed around the tower structure. The main purpose of the clamp is to keep the crane and its load in position on top of the wind turbine. In order to achieve this the clamping force needs to be sufficient. The clamping force is partly generated by the weight of the system and partly by the hydraulic cylinders which can be seen in figure 5.2a. The activated cylinders generate force and press the pads against the tower structure. The last important observation that is discussed is the position of the crane and its load. In the top view the path of the crane tip is indicated with a red circle and an impression of the dimensions of the gearbox are given. To get a better understanding of the working principle, the forces and reaction forces will be examined in the next section.

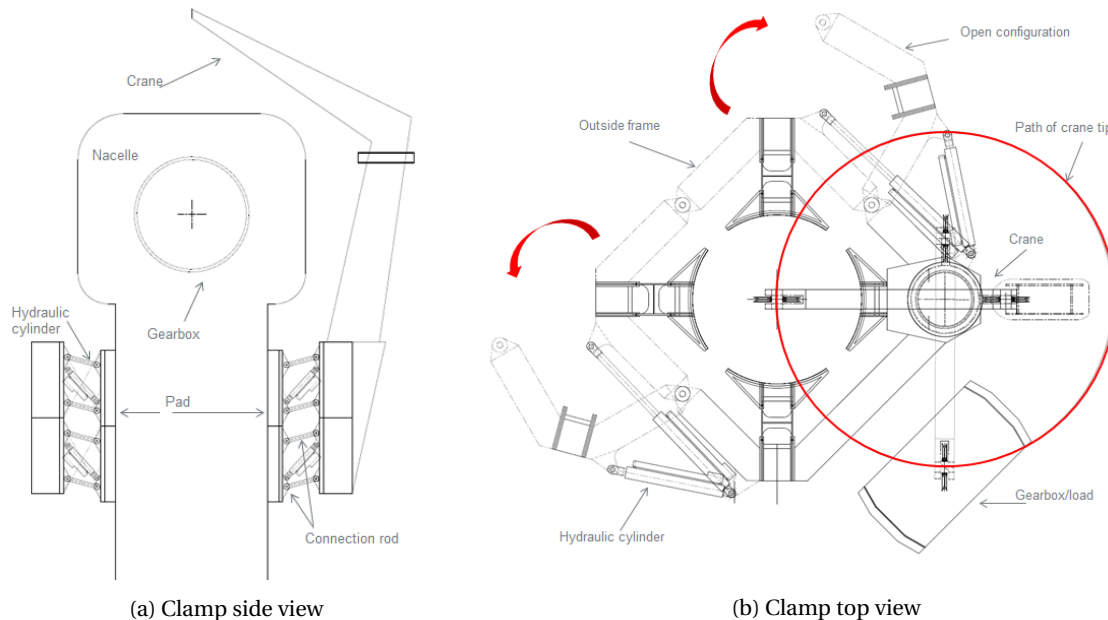


Figure 5.2: Sketches of the clamp

5.2. Clamp Forces and Reaction Forces

In this part the forces and reaction forces of the clamp will be looked at to get more insight in the working principle of the clamp. This is done by analyzing the loads and translate those into reaction forces. The first step is to look at the loads. The system is divided into three masses; (1) clamp, (2) crane and (3) load. In figure

5.3 the centre of gravity (cog) of these loads are indicated. Because the load moves with the location of the crane tip, its centre of gravity is located within the movement area of the crane tip, which is indicated with the red circle. The right figure shows the eccentricity axes of the combined loads. The eccentricity is defined as the distance of the load from the centre of the tower structure. The required x-eccentricity for the lifting operation is eight meters, which follows from the dimensions of the tower and the load as sketched in figure 5.2b.

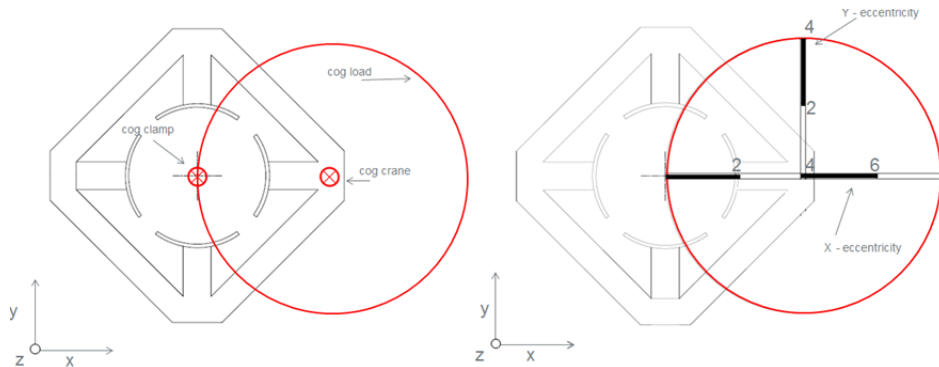


Figure 5.3: Load eccentricity

Now that the location of the loads have been determined, an example is used to look at the magnitude of the forces and reaction forces. The loading conditions are sketched in figure 5.4. A top and side view of the clamp are given. Force F represents the total load as a result from the mass of the structure and the load lifted with the crane. This force can be translated into a moment and a force acting in the centre of the tower structure. For simplification it is assumed that the moment around the y axis (M_y) does not result in reaction forces in pad C and D. This assumption results in higher (conservative) reaction forces in pad A and B, but makes separate analysis of clamp AB and CD possible. The reaction forces at the pad are shown in figure 5.5. The reaction forces for these two systems can be solved by force equilibria, which will be done for the left figure:

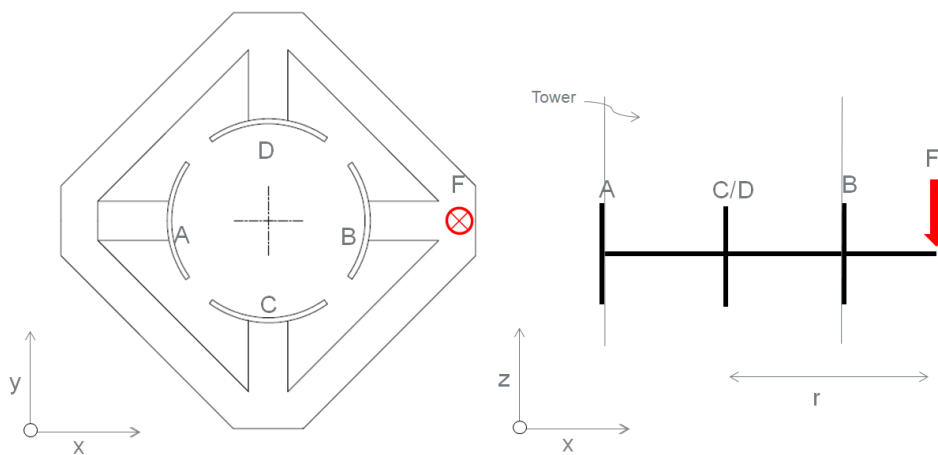


Figure 5.4: Top view and side view of the forces and reaction forces of the tower structure

$$\begin{aligned}
 \sum F_x &= 0, & A_x + B_x &= 0 \\
 \sum F_z &= 0, & A_z + B_z &= F \\
 \sum M &= 0, & M_A + M_B &= M
 \end{aligned}
 \tag{5.1}$$

The system remains its position when the resulting frictional force is high enough. For this set of equations a solution can be found when the system is on the verge of sliding. At that specific situation the following is valid:

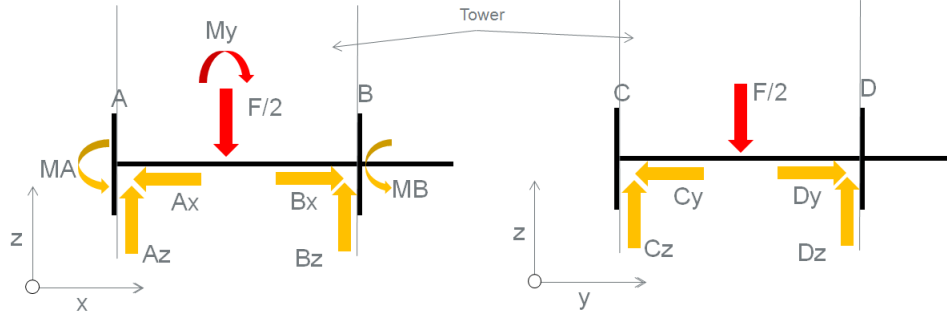


Figure 5.5: Side view of pad A/B (left) and pad C/D (right)

$$\mu A_x = A_z \quad (5.2)$$

$$A_x = B_x \quad (5.3)$$

$$A_z = B_z = \frac{F}{4} \quad (5.4)$$

$$M_A = M_B = \frac{M_y}{2} \quad (5.5)$$

Where μ is the friction coefficient. Now the reaction forces have been determined and the forces can be translated to a reaction force profile. This is sketched in figure 5.6.

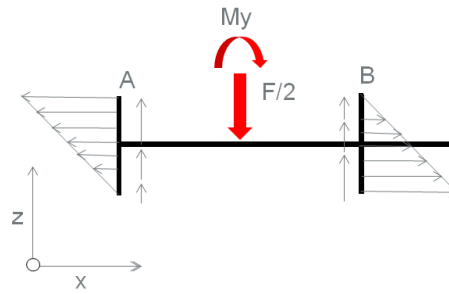


Figure 5.6: Side view of pad A/B (left)

5.3. Safety Factors

In this research the loading capacity of the tower structure will be determined for a variety of pad dimensions. The generated results should be reliable and a safety margin should be included. In order to achieve this three safety factors will be used for correction on frictional force (f_μ), buckling load (f_b) and stress (f_y).

The friction factor is determined following Huisman engineering standards: the friction coefficient (μ) is 0.15. Because the complete maintenance system is kept in place with frictional force, an overestimation of the friction factor can cause hazardous situations, which should be avoided at all times. Therefore a safety factor ($f_\mu = 1.5$) is introduced.

$$\mu_c = \frac{\mu}{f_\mu} \quad (5.6)$$

Here μ_c is the corrected friction coefficient that will be used in this research. To define the loading capacity buckling and stress will be looked at. In this research a linear buckling load is determined using ANSYS. The results should be corrected for non-linear effects (which can be geometric, material and follower loads). The non-linear correction factor (f_{nl}) will be determined in section 7.3.2 by comparing the linear buckling analysis done with ANSYS with results from Eurocode 3: design of steel structures (2007) [1]. The resulting buckling loading capacity (BL) will be corrected as follows:

$$BL_d = BL/f_{nl} \quad (5.7)$$

Where BL_d is the design buckling load. The last safety factor to describe is the one used to correct the stress. The Lloyd code is used for lifting appliances in a marine environment [13]. Normal use is indicated as load case 1, which implies daily operational conditions. The safety factor used for correcting the maximum loading capacity when looking at yield (YL) is 1.5 and is corrected similar to the buckling load:

$$YL_d = YL/f_y \quad (5.8)$$

In table 5.1 an overview of the safety factors is given

Friction	f_μ	1.5
Buckling	f_b	1.7
Stress	f_s	1.5

Table 5.1: Safety factors

5.4. Tower and Load Specifications

The goal of the research is to find a pad configuration such that the tower structure can withstand the load of the heaviest components (gearbox) and crane clamp system. In the next chapters the maximum load will be determined for specific configurations. The dimensions and material properties of the wind turbine tower are used as input and the output is the loading capacity of the tower structure for a specific configuration of the pads. The inputs are given in table 5.2. An indication of the specific load is given in table 5.3 with which the sufficiency of the loading capacity can be checked.

Tower			
Diameter	D	3-6	m
Thickness	t	15-30	mm
Yield strength steel	S355	355	MPa
friction coefficient	μ	0.15	-

Table 5.2: Constants

There is no standard for the wind turbine tower dimensions, they are designed for specific loading conditions which vary for turbine size and location. In this research the 5 MW turbine is used as a starting point. For this specific turbine a diameter of 4 meters and thickness of 20 mm was found. This is based on data from the National Renewable Energy Laboratory [7] (NREL) and Monopile investigation of Thirty [14]. When considering the variable size in wind turbine, the variation in diameter and thickness of investigation is given in table 5.2.

The steel type used for turbine towers is S355 or S235, where the S stands for steel and the number indicates the tensile yield strength of the material. The dimensions of the turbine depend also on the type of steel used. When S235 is used the thickness of the steel also increases [14]. For offshore purposes S355 is more often used¹ and also the NREL turbine investigations work with this type of steel, therefore S355 is used for this research. The friction coefficient has been determined following Huisman engineering standards: the friction factor (μ) is 0.15.

For a 5, 6 and 7 megawatt turbine the weight of the maintenance system and load are given. The mass of the gearbox is estimated following the trend observed in section 2.2.1. The mass of the crane is an estimation based on cranes build by Huisman Equipment, SMST and HEILA. The clamping system mass is an estimation based on the size and required strength of the structure.

¹See for example: Salzgitter steel producer for offshore wind application

Turbine size	5MW	6MW	7MW	Units
Mass gearbox	50	60	70	[mt]
Mass crane	30	40	50	[mt]
Mass clamp	20	30	40	[mt]
Total mass	100	130	160	[mt]

Table 5.3: Load estimations

5.5. Variables of Interest

In the previous sections a preliminary design of the clamp and its working principle were given. This information is used to define the variables of interest in this section. The lay-out of the contact surface influences its performance, therefore the focus is on the determination of the properties and dimensions of this contact surface. The following variables are identified; elasticity of contact layer, number of pads, width and height of the pad. Furthermore the dimensions of the tower structure also influence its loading capacity. Therefore also the influence of diameter and thickness of the tower will be investigated.

5.5.1. Elasticity

The clamp transfers the forces to the tower structure and to distribute these forces, a well-fitting connection is required. In figure 5.7 a top view of a pad and the support structure can be observed, where the pad is touching the tower structure. The frame is made of construction steel, but to assure the clamp is not damaging the tower, the contact surface is made elastic material. By doing so the load will be distributed more equally on the tower structure². For the elastic layer polymers or elastomers can be used. The chemical composition of

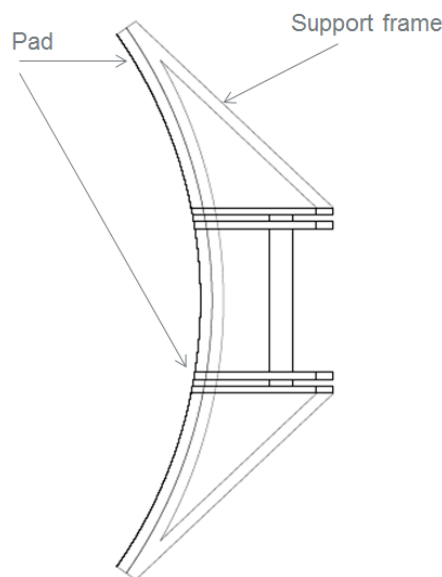


Figure 5.7: Top view support frame and pad

this material groups is of minor importance, but the elastic properties are. The elastic layer can be made with varying material properties, such that it suits the purpose of distributing the forces and generating friction. When long segments are used, the material will be elastic and a high amount of crosslinks result in more rigid polymers.

The rigidity of the material, given by the elastic modulus (E-modulus) determines its behaviour. Therefore for this research the effect of this parameter will be investigated. So for the modelling part the elastic modulus of the PU is of importance which can vary from 10-3000 Mpa [3]. The great variation of these material properties is its strength and therefore often developed for similar purposes in the offshore industry³.

²It should be noted that also the clamp structure can be designed as flexible by changing the material thickness. This type of solution is excluded from this research, a detailed design is needed from the pad to do this adding a pad on the structure is a simple and often used solution in the offshore industry

³For example Ridderflex and BIS are companies which make polyurethane pads for the offshore industry

5.5.2. Number of Pads

The number of pads is also a variable of investigation. Here the focus will be on mapping the effect of increasing the number of pads that is used on the tower structure. However, it should be noted that there are also technical boundaries that limit the number of pads; by adding more pads, the system also increases in complexity. Before the decision is made the focus will be on mapping the effect of increasing the number of pads.

5.5.3. Width and Height

The width and height of the pad can be considered vital variables and will be looked at simultaneously. Where the definition of height (H) and width (W) is illustrated in figure 5.8. These variables will be discussed simultaneously, because for both variables the area of the pad is increased and therefore it is interesting to evaluate and compare those results and see what the effect is on the loading capacity. Here width is given as an angle in degrees and height in meter.

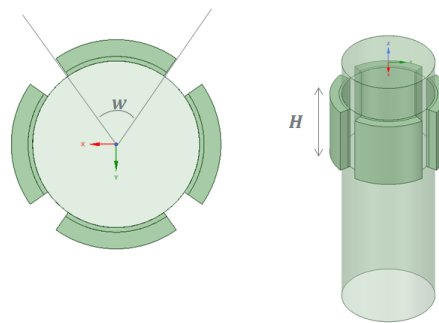


Figure 5.8: Definition of pad width and height

5.5.4. Diameter and Thickness of the Tower

The thickness and diameter of tower vary for different types of turbines. The maintenance system should also work on these turbines, therefore also the loading capacity for varying diameter and thickness will be investigated.

5.6. Conclusion

In this chapter a preliminary design of the clamp have been presented. This consist of a frame with pads that are clamped against the tower structure using hydraulic cylinders. By simplifying the structure the reaction forces and moments have been determined. Furthermore, safety factors, tower- and load specifications have been presented which are listed in table 5.4. In the last section the variables of investigation have been given. In the next chapter this will be used as the input for the research setup.

sf friction	f_{μ}	1.5	[-]
sf buckling	f_b	1.7	[-]
sf yield	f_y	1.5	[-]
Diameter tower	D	3-6	[m]
Thickness tower	t	15-30	[mm]
Steel strength tower	S355	355	[Mpa]
Friction coefficient	μ	0.15	[-]
x-eccentricity	e	8	[m]
Load 5 MW turbine	-	100	[mt]
Load 6 MW turbine	-	130	[mt]
Load 7 MW turbine	-	160	[mt]

Table 5.4: Overview of specifications and factors

6

Finite Element Model

For all properties a finite element modelling (FEM) analysis is executed. ANSYS workbench 17.2 is used for this purpose. The focus will be on using of this program; the variables will be translated into a simulation setup. Furthermore, the pre-processing and solving method of the FEM software will be discussed. In the pre-processing part the geometry, mesh and boundary conditions will be discussed. Thereafter the solving method will be described.

6.1. Variables

6.1.1. Elasticity

The next step is to make the translation from the search for the right properties into an simulation setup. For these simulations a quarter of the full tower clamp configuration is used. Since the model (and the loading pattern that is used for this purpose) is symmetric this quarter model is used to reduce computational time. In section 6.2 the configuration of the model is described more thoroughly. Several simulations will be executed where the E-modulus is varied in the range of 10-10000 Mpa. A uniform pressure of 0.4 Mpa will be applied on the pads. Because a linear analysis is done, the magnitude is of minor importance (the resulting stress will increase linearly with the applied load).

The results of the simulation will be inspected qualitatively on stress distribution, meaning that the stress distribution on the tower will be looked at in detail. This is done because especially the location of the stresses are of importance.

The conditions for these simulations are listed in table 6.1. For these simulations a pad height of three meters used, width of 70 degrees and four pads. To reduce complexity of the simulation the eccentricity is set to zero. By doing so the load on the pads can be simplified by a constant pressure working on all pads. A rubber thickness of 110 millimetres is used, corresponding to the thickness of pads used in the industry. Furthermore the tower diameter and thickness from a 5 MW turbine are used as input for the model.

Conditions		
Pad height	3	[m]
Pad width	70	[deg]
Number of pads	4	[-]
Eccentricity	0	[-]
Rubber thickness	110	[mm]
Rubber elasticity	variable	[Mpa]
Diameter tower	4	[m]
Thickness tower	0,02	[m]

Table 6.1: Conditions for elasticity simulations

6.1.2. Number of Pads

To map the effect of increasing number of pads, there will be looked at a variety of pad widths and number of pads which can be seen in table 6.2. Here the selection for N=3 is chosen as a starting point¹, followed by N=4. Thereafter the number of pads is doubled such that the effect of a large number of pads can be investigated. By doubling the number of pads at different pad width (20, 40, 60, 70 and 80 degrees), a comparison can be made between situations where the total coverage of the circumference is the same, but the number of pads varies. By doing so a comparison between the effect of widening the pad and increasing the number of pads can be done.

In table 6.3 the conditions for the simulations are listed. Also here a pad height of three meters is chosen and no eccentricity of the load is used in the model and the rubber thickness has the same value as used in the elasticity model setup. Furthermore an E-modulus of 1200 MPa is used, which show favourable material behaviour (this will become clear after studying the results of the elasticity simulations). Also here the tower dimensions of a 5 MW turbine are used.

Number of pads	Pad width [deg]
3	20,40,60,70,80
4	20,40,60,70
8	20,40
12	20

Table 6.2: Width and number of pads that will be modelled

Conditions		
Pad height	3	[m]
Pad width	variable	[deg]
Number of pads	variable	[-]
Eccentricity	0	[-]
Rubber thickness	110	[mm]
Rubber elasticity	1200	[Mpa]
Diameter tower	4	[m]
Thickness tower	0,02	[m]

Table 6.3: Conditions for variation in number of pads

6.1.3. Width and Height

By increasing the width and/or height it the loading capacity will increase. It is of importance to check how the loading capacity will evolve by varying these parameters. In the previous sketched simulation descriptions no eccentricity of the load was included to reduce complexity of the model. Here the eccentricity is included, such that insights can be gathered in the loading capacity for realistic loading conditions. Furthermore the width is varied from 60-80 degrees and the height is varied from 2-5 meters as can be seen in table 6.4

In table 6.5 the conditions are listed. Here the same conditions are used as mentioned in the previous simulation setups: number of pads used is four, rubber thickness is 110 millimeters, E-modulus of the rubber is 1200 Mpa and the dimensions of a 5 MW turbine are used as input.

Width [deg]	x-eccentricity [-]	Height [m]
60	0-4	2,3,4,5
70	0-4	2,3,4,5
80	0-4	2,3,4,5

Table 6.4: Simulation configurations for pad height and width

¹here N=2 is excluded, since this setup results in an unfavourable composition to deal with the moment force in x direction (see figure 5.3)

Conditions		
Pad height	variable	[m]
Pad width	variable	[deg]
Number of pads	4	[-]
Eccentricity	variable	[-]
Rubber thickness	110	[mm]
Rubber elasticity	1200	[Mpa]
Diameter tower	4	[m]
Thickness tower	0,02	[m]

Table 6.5: Conditions for variation in number of pads

6.1.4. Diameter and Thickness

The last step is to get insight in the loading capacity for varying tower diameter and thickness. Here the 5 MW turbine was used as a starting point and because the size of the turbines installed is increasing the range of investigated dimensions is as follows: diameter of 3-6 meters and a thickness that come with this these tower size as can be seen in table 6.6.

The conditions are listed in table 6.7. Also similar clamp configurations are used as in the elasticity simulations and an E-modulus of 1200 Mpa is used for the rubber pad.

D tower [m]	t [mm]
3	14-28
4	16-30
5	18-32
6	20-34

Table 6.6: Simulation configurations for varying tower diameter and thickness

Conditions		
Pad height	3	[m]
Pad width	80	[deg]
Number of pads	4	[-]
Eccentricity	0	[-]
Rubber thickness	110	[mm]
Rubber elasticity	1200	[Mpa]
Diameter tower	variable	[m]
Thickness tower	variable	[m]

Table 6.7: Conditions for variation in number of pads

6.2. FEM pre-processing

When making a model, the goal should be defined clearly such that design choices can be made and the desired results will be found. In this case the goal is to get insight in the effects of certain loading conditions on the tower structure for different clamp configurations. In this part the geometry, element type, mesh and boundary conditions will be discussed to give insight in the simulation setup.

6.2.1. Geometry and Element type

The geometry is the (simplified) structure used as input in the FEM program, ANSYS workbench in this case. For this purpose the CAD software Spaceclaim is used. As mentioned in the introduction a simplified model is made, which can be seen in the figure below:

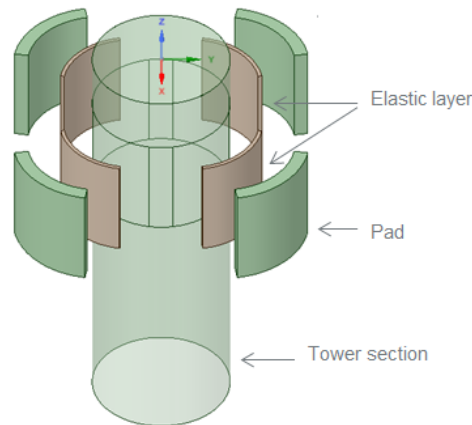


Figure 6.1: Spaceclaim geometry exploded view with 4 pads

This figure is a simplification of the clamp and is modelled as such, because the goal is to get insight in the effect of certain loading conditions on the tower structure. The configuration therefore just exist of three different parts; (1) the tower section with topplate, (2) pads with the (3) elastic layer. With this setup the complexity is reduced to the minimum necessary and loads can be applied on each pad separately. A combination of shell and solid elements have been used to do so. In the next paragraphs the modelling of these three parts will be explained.

The wind turbine tower is modelled as a twelve meter long cylinder with a rigid plate on top. The nacelle is replaced in the model with a plate, which assures the top to behave like a rigid structure. This assumption can be done, because the nacelle is attached to the tower structure with a connection part and a yaw bearing of which the steel structure dimensions exceed those of the tower thickness. Therefore the top of the tower can be considered a rigid structure.

As can be seen in figure 6.1 only a section of the tower is modelled. This is the largest part of the model and its size influences the computational time, therefore the tower section must be kept as short as possible. However, when the section is too short the model does not describe the behaviour of a wind turbine tower. Its performance has been evaluated to find the right dimensions of the tower structure (see section 7.1.1). For the tower section shell elements are used, which are well suited to model plates and non-massive structures[15]. Shell elements assure a acceptable computational time and accurate result for thin walled structures.

The pad is modelled as a rigid part and solid elements are used to do so, because the structure cannot be considered thin-walled.

The elastic layer can be seen in figure 6.1 and is modelled as a curved plate, 110 mm wide. In reality this material will be added in strokes or block on the pad, such that there is space for the flexible material to extend perpendicular to the load direction. However, in this case we are interested in the effect on the tower structure and therefore it is simplified as a solid element.

6.2.2. Mesh

Now the shape is defined, the refinement of the mesh should be discussed. The size of the elements should be such that all the details of the displacements and stresses are covered in detail, but again; computational time should be minimized. To assure this is done the mesh is refinement at locations where the stress/displacement gradients are high as can be seen in the figure below:

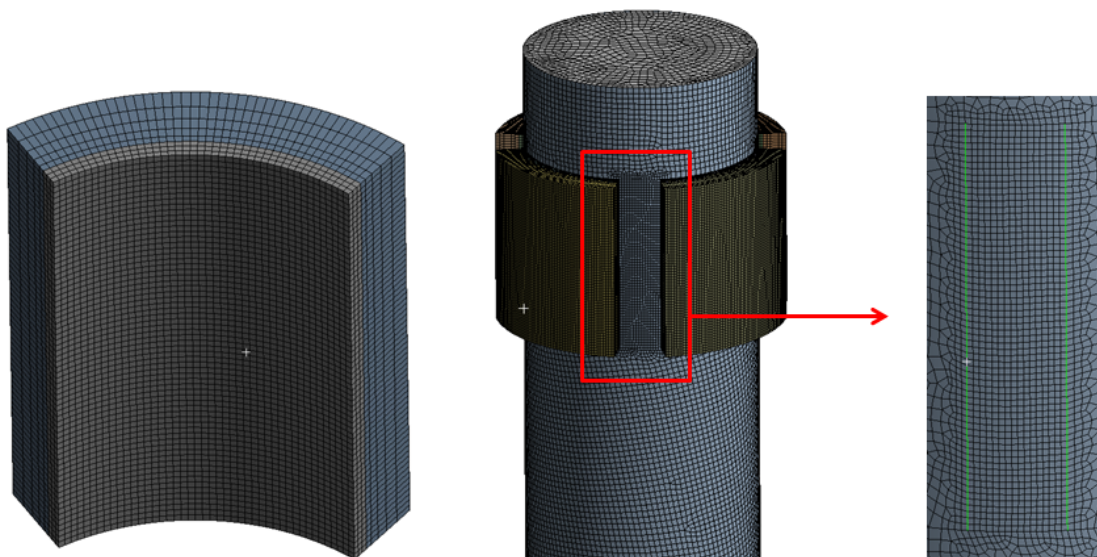


Figure 6.2: Mesh configuration of the model. The green lines indicate the imprint of the pad edges

The most left figure shows the pad and the elastic layer. Here it can be seen that the mesh becomes more refined when moving toward the elastic layer and on this layer the elements are the smallest. Here the mesh is of significant importance since the forces are transferred from the rigid part onto the tower structure. Therefore the stresses and displacements have to be detailed and the mesh must be refined. The same applies to the places where the pad is in contact with the tower. The highest stress gradients are expected on the edges of the pad and on the area in between the gap. In figure 6.2 it can be observed that, because of these expected high stress/displacement gradient the mesh is refined on the indicated red area.

There are several methods and tools to inspect the mesh quality, which have been used complimentary. First the skewness can be checked, which is a measure of mesh quality, where the shape of the different elements is evaluated and therefore it is not necessary to run a simulation for this check (only the mesh needs to be defined). Secondly, when a simulation is performed it is possible to check the energy error². In combination with visual inspection this method is used to improve the mesh at locations where the error is large or the stress gradient development is not fluent. Finally the mesh size can be adjusted and the changes in the stress results are used as final check; when mesh converges and stresses do not change significantly, than the mesh quality is acceptable as was tested for the configuration in figure 6.2. In appendix ?? details of these checks can be found.

6.2.3. Boundary Conditions and Loads

Defining the boundaries of a model is of importance, since finding a solution with FEM is solving a boundary value problem. The selection of the boundary conditions influences the results and obviously should be chosen with care. Keeping a structure and its boundary conditions as simple as possible is one of the most important general rules using FEM. In this research this has been chosen as a starting point.

²The basic idea of this method is that the difference between the average stress and the interpolated stress at a node is used to calculate the energy error of the structure. It can easily be understood that when the mesh is very coarse, the energy error will increase.

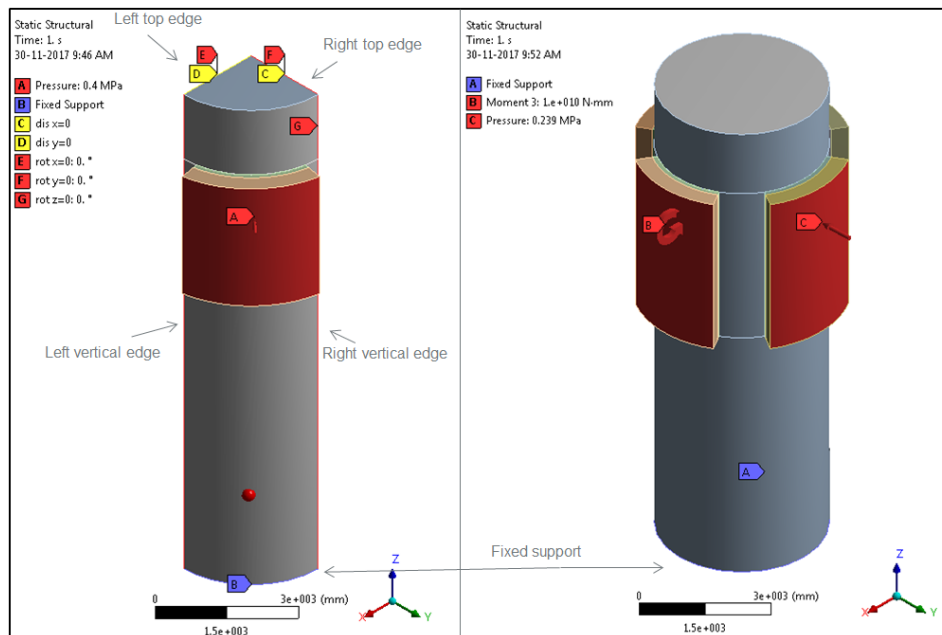


Figure 6.3: Boundary conditions and loads for the full model (right) and a quarter model (left)

In the figure above two models can be seen. First the full model will be discussed. On the right side the full model is given where the boundary conditions are also indicated. The bottom end is fixed (indicated with the blue label) and the top end is free. As shown in section 6.2.1 the modelled section is of sufficient length, such that the stresses in the structure are not influenced by the location of the clamped end. The top end is free to move, which corresponds to the situation of the wind turbine. Two types of loads are used in the simulations: pressure and moments, which are applied on the outside of the pad, on the area indicated in red in figure 6.3. In reality there are also loads from the nacelle, and the weight of the system. The influence of these loads on the buckling effect and the stress where found to be small and therefore are neglected in the calculations. In appendix ?? the calculations for these assumptions can be found.

In several simulations only a constant pressure is applied as a load. In these cases the model is symmetrical and therefore can be simplified. On the left side of figure 6.3 only a quarter of the full model is given and represents the full model for uniform loading conditions. This simplification reduces the computational time significantly. The only difficulty in using this quarter model is applying the right boundary conditions to assure the same results will be found when using the full model. The following rotations and displacements where fixed to do so:

	Displacement = 0	rotation = fixed
Left top edge	y	x
Right top edge	x	y
Left vertical edge	y	z
Right vertical edge	x	z

Table 6.8: Applied boundary conditions for the quarter model

6.3. FEM - solution

The result that are subject of investigation are the stress and the buckling load. In this section the von Mises stress and the Linear buckling analysis will be described. In the next chapter the focus will be on the validation of these solutions.

6.3.1. von Mises stress

The von Mises stress is used as an indicator for plastic deformation of material subjected to multidimensional stresses. When stress from one direction is applied to a material, the stresses should be below the yield stress to avoid yielding. When the stresses work in multiple directions, an approximation criterion should be used.

In ANSYS workbench the von Mises criterion is used for this purpose:

$$\sigma_{vm} = \sqrt{\frac{1}{2}((\sigma_{xx} - \sigma_{yy})^2 + (\sigma_{yy} - \sigma_{zz})^2 + (\sigma_{zz} - \sigma_{xx})^2) + 3(\tau_{xy}^2 + \tau_{yz}^2 + \tau_{zx}^2)} \quad (6.1)$$

6.3.2. Linear Buckling Analysis

In this study the focus will be on circumferential buckling, which is buckling as a result of the force exerted on the tower circumference. This is a logical starting point, since the 'squeezing' force which is used to assure the clamp and the system stays in place, is high in comparison to the thin shell structure. One can compare this effect with squeezing a soda can, which can easily be done, where the soda can is able to carry high loads that are placed on top. Another reason for this approach is that the maintenance will only be done in mild environmental conditions and the wind turbine won't work at the moment of maintenance. This means that the loads (mainly vertical) won't be near the limits of the structure. Therefore a logical first step is to look at the circumferential buckling

The linear buckling analysis done in ANSYS consist of the following three steps: (1) a load is applied to the structure which is used as a reference. (2) Then a linear static analysis is carried out to obtain stresses that are needed to form the geometric stiffness matrix K_g . (3) Finally the buckling load can be calculated as part of the second load step, by solving the eigenvalue problem:

$$(K - \lambda K_g)x = 0 \quad (6.2)$$

Where K is the stiffness matrix of the structure and λ is the multiplier of the reference load. x represents the eigenvector which correspond to the eigenvalue. ANSYS uses the Lanczos method to solve this eigenvalue problem (see for example Rajakumar and C. and Rogers [12]). Since the lowest eigenvalue is associated to buckling, only the first eigenvalue will be calculated. The buckling load will be given as:

$$F_{crit} = \lambda_{ult} F_{ref} \quad (6.3)$$

In our case the multiplier λ will be the unknown such that

$$\lambda_{ult} = F_{crit} / F_{ref} \quad (6.4)$$

The F_{ref} is given as the load that is applied on the tower by the clamp and λ_{ult} is the result given by ANSYS.

7

Model Verification

The modelled system exist of three parts: the (rigid) pad, a rubber layer and the tower section. In this part the model will be verified to assure the modelling of these parts is done correctly. By doing so irregularities in the simulating process can be found and corrected. Three steps will be followed:

1. Checking geometric and loading assumptions. Here the mesh and the simplifications of the model are checked (section length tower and loads)
2. Verification of stress analysis. Here the linear stress analysis assumption will be checked and a method to compare results with analytic results will be presented.
3. Verification of linear buckling analysis. Here the following question will be answered: how can the linear buckling analysis be applied correctly?

Length tower section			
Tower length [m]	σ_{vm} [Mpa]	Change [%]	
10	259.02	-	
11	262.78	1.43	
12	266.12	1.25	
13	266.26	0.05	
Loading assumptions			
Vertical loads	σ_{vm} [Mpa]	Change [%]	
Yes	138.48	-	
No	137.5	0.73	
Deflection			
Configuration	$l_1 \sin(\theta)$ [mm]	$l_1 \theta$ [mm]	δ [mm]
N=4,D=4,W=70,t=15	4.801	4.805	4.8
N=8,D=4,W=20,t=20	4.100	4.100	4.1
N=4,D=4,W=20,t=20	11.400	11.399	11.4

Table 7.1: Verification model

7.1. Geometric and loading

7.1.1. Length tower section

Here is checked weather the right tower section length is modelled. This is done by increasing the pipe length and check the von Mises stress for consecutive pipe length cases. To verify the pipe length the following pad configuration was used: N=4, D=4m, t=20mm, W=70 deg, H=5m. Here the longest pad dimensions were chosen, because when a workable configuration is found for the longest investigated pads, the tower section will also be long enough for the shorter pads. In table 7.1 the maximum observed von Mises stress is given for increasing length of the tower section. Here it can be seen that the maximum stress is converging and not minimum change is observed for a modelled tower length of 13 meters. Therefore 12 meter is assumed to be sufficient and this will be used in the modelling process.

7.1.2. Loading assumptions

Excluding vertical loads and moment (caused by the nacelle and the clamp) can reduce complexity of the model. These loads can only be neglected if the effect on the resulting stresses are small and therefore need to be investigated. This is done by comparing the results of two cases: (1) top load and clamp load are applied on respectively the tower section and clamp and (2) the setup where only a clamping load is applied¹. The resulting stresses are listed in table 7.1. The difference between the observed maximum von Mises stress are small (i.e. smaller than one percent) and therefore these vertical loads are assumed to be negligible.

7.2. Stress

7.2.1. Linear stress analysis

Linear static stress analysis can only be done when geometric non-linearity's are negligible. This can be assumed when the deformations are small. Material non-linearity's are neglected. Material non-linearity's are in place, but these effects are generally small and of greater importance when looking at non-linear materials like plastic and rubber. In our case the deformation of the PU is not of interest and therefore are not investigated

The deflection for 4 cases has been investigated and with high expected deflection (low thickness and large gap). The deflection is within acceptable boundaries when $\sin(\theta) \approx \theta$ and $\cos(\theta) \approx 1$ where θ is defined in figure 7.1. The results are presented in table 7.1. Here it can be seen that the difference between $l_1 \sin(\theta)$ and $l_1 \theta$ are very small and therefore the small deflection assumption is acceptable.

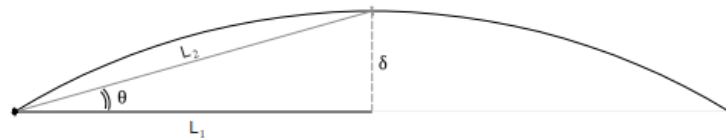


Figure 7.1: Sketch of deformed area between the pads

7.2.2. Hoop stress

The stress calculations with FEM will be verified by comparing the analytic determined hoop stress (or circumferential stress) with the stress as found in the ANSYS model.

Calculation

For a thin walled pressurized cylinder pressure the hoop stress (σ_h) can be calculated analytically:

$$\sigma_h = P \frac{D_{out}}{2t} \quad (7.1)$$

Where P = pressure exerted on the cylinder and t = shell thickness. In the situation of investigation the stress is not applied fully circumferential and therefore the determination of the hoop stress needs to be adjusted.

¹for the top structure a load of 440 mt is used, which is based on the specifications of the 5 MW RE-power turbine (see appendix H. For the clamp and crane system a load of 100 mt is used, following the load estimations in table 5.3.

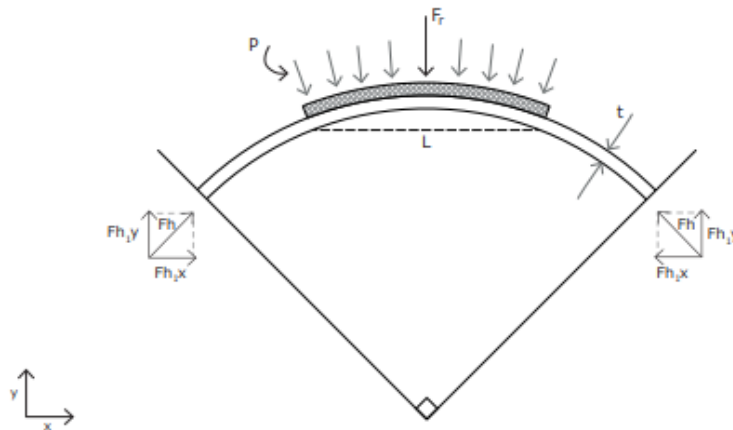


Figure 7.2: Sketch of quarter pipe model

$$2F_{h,y} = F_r \quad (7.2)$$

Where F_r is the resulting force of the pad pressure P and F_h is the resulting force of the hoop stress

$$\frac{2\sigma_{hoop}ht}{\sqrt{2}} = Plh \quad (7.3)$$

Now the σ_h can be written as:

$$\frac{Pl\sqrt{2}}{2t} \quad (7.4)$$

The stresses that occur in the wall are a hoop and bending stresses. The maximum principal stress will be found on the outside (hoop and tensile stress) and the minimum stress occurs on the inside (hoop and compression stress). In this verification we are only interested in the hoop stress which will be calculated as the average of those two values:

$$\frac{\sigma_{outside} + \sigma_{inside}}{2} \quad (7.5)$$

Where l is calculated as a function of the pad width (W , in degrees):

$$l = 2r \sin\left(\frac{W}{2}\right) \quad (7.6)$$

When comparing the analytic and the FEM results, it should be noted that the hoop stress differs over the height. The hoop stress in the tower has a peak at the middle of the pad height and the stress flow is reducing when moving away from this center.

Results

The hoop stress is determined analytic and compared with the FEM results. In chart 7.3a the results for a specific case can be observed. Here the hoop stress is given for $D=3\text{m}$, $N=4$ and $W=70$ deg (results from other dimensions can be found in appendix C. When studying the chart it can be observed that both lines follow the same trend and the resulting stress is of the same order. However, the hoop stress as found in ANSYS is higher for all cases. This observation can be explained by looking at figure 7.3. Here the von Mises stress is shown for five location on the tower. The stress is varying over the height, where a peak can be observed at the horizontal plane that is crossing the middle of the pad. When moving away from this point the stress is decreasing. The hoop stress as given in char 7.3a is determined from the highest value and therefore it is higher than the analytic hoop stress.

Conclusion

When comparing the analytic and FEM results comparable stresses can be found. Therefore it can be assumed that the modelling is done correctly.

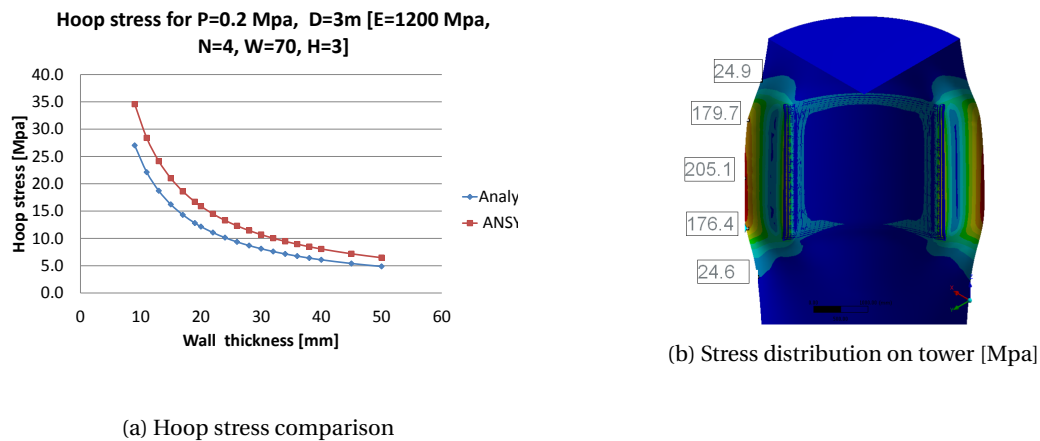


Figure 7.3: Stress resultstress results

7.3. Buckling Analysis

In this section the buckling analysis with ANSYS is compared with European standards as given in Eurocode 3: Design of steel structures - part 1-6: strength and stability of shell structures [1]. The FEM simulation and the Eurocode results can only be compared when the same setup is used. This setup is presented in figure 7.4 and differs considerably from the clamp tower setup. In this figure a top view and side view is given of the Eurocode setup. The arrows indicate a constant pressure that is applied on the cylinder. The loading profile differs on two points from the clamp tower setup: (1) the loading profile is variable in height and (2) the load is applied only on a section of the tower, where the Eurocode buckling calculations a uniform pressure is applied on the full length of the shell.

Despite these differences in loading conditions, the tower structure is similar and therefore it can still be used to gather valuable insight for the buckling analysis. In particular insights can be gathered on the differences with the linear buckling analysis and a realistic buckling load where material quality and a safety factor is included. Therefore in this section the Eurocode buckling load will be compared with the buckling load given by the ANSYS model. This will be done for variable height of the tower section (indicated with H in figure 7.4). Before this comparison can be made the eurocode approach will be described in the next section.

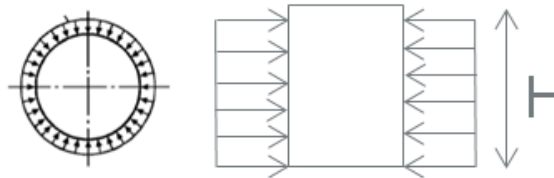


Figure 7.4: top and sideview of loading conditions following Eurocode 3

7.3.1. Eurocode Circumferential Buckling Pressure

The Eurocode buckling strength is calculated by the following steps [1] :

- Elastic buckling strength is determined ($\sigma_{\theta, Ecr}$)
- Then the relative slenderness (λ_{θ}) can be found
- The reduction factor (χ_{θ}) can be determined, where the relative slenderness, plastic range and imperfection are included
- Finally the ultimate buckling stress and the buckling pressure can be calculated

Elastic buckling strength The length of the shell segment should be characterized in terms of the dimen-

dimensionless length parameter ω :

$$\omega = \frac{l_c}{r} \sqrt{\frac{r}{t}} \quad (7.7)$$

Here l_c is the length of the cylinder, r the radius and t the thickness. For this research we only looked at medium length cylinders which are defined by²:

$$1.7 \leq \omega \leq \frac{r}{t} \quad (7.8)$$

The elastic circumferential buckling stress is obtained from:

$$\sigma_{\theta,Ecr} = E \frac{C_{\theta}}{\omega} \frac{t}{r} \quad (7.9)$$

Where C_{θ} depend on the boundary conditions and can be obtained from the following table (Where BC 1 is clamped, BC 2 is pinned and BC 3 is free):

Case	Cylinder end	Boundary condition	Value of C_{θ}
1	end 1	BC 1	1,5
	end 2	BC 1	
2	end 1	BC 1	1,25
	end 2	BC 2	
3	end 1	BC 2	1,0
	end 2	BC 2	
4	end 1	BC 1	0,6
	end 2	BC 3	
5	end 1	BC2	0
	end 2	BC3	
6	end 1	BC 3	0
	end 2	BC 3	

Figure 7.5: Boundary Conditions source: Eurocode

Relative slenderness

$$\lambda_{\theta} = \sqrt{\frac{f_y}{\sigma_{\theta,Ecr}}} \quad (7.10)$$

Reduction factor

$$\chi_{\theta} = 1 - \beta \frac{(\lambda_{\theta} - \lambda_0)}{(\lambda_p - \lambda_0)} \text{ for } \lambda_0 < \lambda_{\theta} < \lambda_p \quad (7.11)$$

$$\chi_{\theta} = \frac{\alpha}{\lambda_{\theta}^2} \text{ for } \lambda_p < \lambda_{\theta} \quad (7.12)$$

Where α is the elastic imperfection reduction factor $\beta = 0.6$ is the plastic range factor and $\lambda_0 = 0.4$ is the relative slenderness squash limit.

$$\lambda_p = \sqrt{\frac{\alpha}{1 - \beta}} \quad (7.13)$$

Ultimate buckling stress

$$\sigma_{\theta,Rd} = \frac{\chi_{\theta} f_y}{\gamma_m} \quad (7.14)$$

Where γ_m is the partial factor which is 1.1 following Eurocode procedure. Now the corresponding pressure can be found:

$$P_{cr} = \frac{4\sigma_{\theta,Rd} t}{D} \quad (7.15)$$

²in this research all tower sections modelled meet the requirements for medium length cylinders.

Important to note here is that the buckling pressure is linearly dependant on the length of the cylinder when $\lambda_p < \lambda_\theta$ (equation 7.12). This means that the total buckling force is constant when $\lambda_p < \lambda_\theta$. The investigated tower sections are within this range and therefore it is interesting to check if this same trend is observed for the clamp/tower setup. This will be done in section 8.3. First the focus is on the comparison of the Eurocode results when the same setup is modelled in ANSYS.

7.3.2. Results comparison Eurocode with ANSYS simulations

The ANSYS simulation results present a linear buckling limit, or in other words; a theoretic (upper) limit for the buckling load. In figure 7.6 three graphs can be observed: (1) the buckling red line representing the Eurocode buckling pressure, (2) the green line showing the ANSYS buckling pressure and (3) the blue line which gives a corrected ANSYS buckling pressure.

First the focus is on the red and green line. It can be seen that the ANSYS buckling pressure and the Eurocode buckling pressure follow the same trend when the height of the modelled section is increased. However, the ANSYS results is substantially higher than the buckling pressure resulting from the Eurocode. The ANSYS model gives a theoretic upper limit, in reality failure will occur before this limit is reached. This is the result of non-linear behaviour (material, geometric or load non-linearity's). In the used Eurocode partial safety factors are used to correct for this behaviour. When we want to use the buckling results also a safety factor should be introduced to correct for this non-linear behaviour. The next step is to identify the safety factor that is used for the Eurocode calculations and also use this same safety factor for the ANSYS results.

In the used Eurocode a correction factor for material quality ($\alpha = 0.75$) was introduced and a reduction factor ($\gamma_m = 1.1$) is included (see equation 7.12 and 7.14). When combing these safety factors a combined safety factor can be found:

$$f_b = \frac{\gamma_m}{\alpha} = 1.5 \quad (7.16)$$

When we want to compare these results from the ANSYS anaysis and the Eurocode, the same safety factor should be used. The blue line shows the result when also for the linear buckling analysis this safety factor is used. It can be seen that the blue and the red show similar results and so it can be concluded that these safety factor are the missing link between the used Eurocode and the ANSYS simulation results.

It should be addressed that a slight difference is observed between the Eurocode and the corrected ANSYS results. For short cylinders the ANSYS buckling pressure is more negative than the Eurocode, but this difference fades when the height of the tower section is increased and finally the ANSYS results is slightly more positive than the Eurocode result. However, this difference is small (within 2%) and therefore the resulting ANSYS and Eurocode are comparable. Having said this, it can be concluded that the buckling load deter simulations can be useful tool to estimate the buckling load

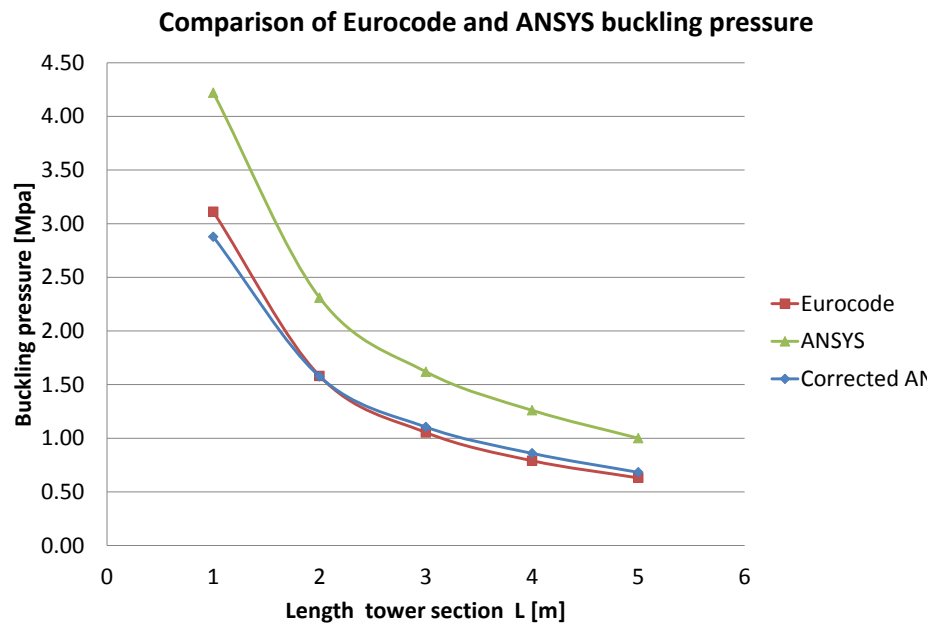


Figure 7.6: Eurocode and ANSYS buckling pressure results for uniform circumferential applied pressure

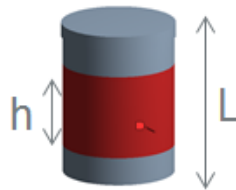


Figure 7.7: Pipe section. Red area indicates the pressurized area

7.3.3. Convert uniform loading profile

In this section the translation will be made from a uniform pressure to a variable pressure in (1) meridional and (2) circumferential direction. The first one to discuss is Weingarden (1962), who looked into pipes with linearly varying pressure in longitudinal direction and a uniform pressure circumferential as illustrated below:

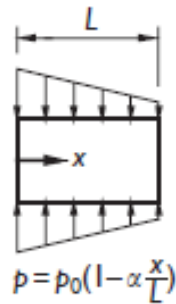


Figure 7.8: Source: Weingarden, 1962

In this research he compared a pipe where the pressure varied linearly with a pipe with a uniform pressure. In the last case the pressure was $\frac{1}{2}P_{max}$. The maximum variation in buckling pressure was less than 5%. This result shows that the case of varying pressure can be simplified: the varying pressure can be replaced by a uniform pressure.

When looking at circumferential variation of pressure, two sources were identified which give insight in the effect of variable pressure when determining the buckling pressure. The first method is given in eurocode EN-EN-1993-1-6 (2007) [1], where a method is presented to find an equivalent uniform pressure for a situation where the pressure is varying on the circumference as sketched in figure 7.10. It can be seen that for a variable circumferential pressure is transformed into a constant pressure, where a transformation factor (k_w) is used to determine the constant equivalent pressure. However, this method is used for silo's and thin shells, where the pressure is a result of the wind conditions. As can be seen in figure 7.10, this specific situation where a peak pressure is observed on a very small area and on the remaining area a negative pressure is observed. This pressure pattern does not show similarities to the loading patterns of the clamp and therefore this method cannot be used in the case of investigation. What can be learned from this method, however, is that the value of the equivalent pressure is lower than the peak pressure observed ($0.65 \leq k_w \leq 1$).

The second research of interest is done by Almroth [2], who investigated the effect of circular varying band pressure on the buckling pressure as can be seen in figure 7.9. Where the variation in pressure is translated to a factor, the skew factor ρ , where ρ has a value from zero to one and $\rho = 0$ for a uniform pressure and increases for increasing cosine variation in pressure. Almroth observed a rise in buckling pressure for increasing skewness. Also this configuration of pressure does not look similar to the loading condition of this investigation, however here is observed that the maximum pressure increases when the pressure is not uniform and this can be a valuable when checking the results from ANSYS.

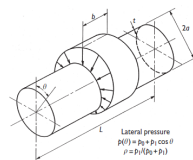


Figure 7.9: Source: Almroth, 1962

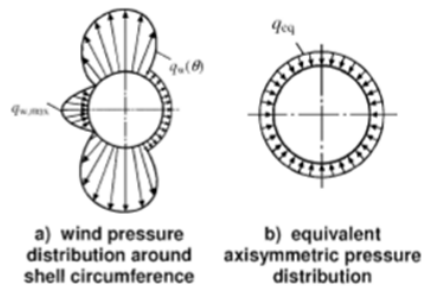


Figure 7.10: Source: eurocode EN-EN-1993-1-6 (2007)

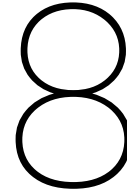
7.4. Conclusions

First the model geometry and loading assumptions have been checked. It has been determined that modelling a section of twelve meters in length should be sufficient to assure boundary effects do not influence the results. The vertical load has been shown to be negligible.

Secondly the stress results from the model have been verified. It was shown that the hoop stress results of the model were comparable with the analytically expected results. Thereby the stress analysis is verified.

Thirdly the results from the buckling analysis have been checked with analytical values. The exact same setup as put into the ANSYS model has been evaluated analytically. The same trend was identified, but the analytical results were found to be lower for a variation in tower lengths. This difference is explained as the theoretical upper limit of buckling and all non-linear effects are neglected (material and geometric non-linearity).

In the comparison part a difference has been observed between the results based on the Eurocode formulation and the results that are produced using ANSYS workbench. When the linear buckling load is used it should be corrected for the non-linear effects. A safety factor can be introduced in order to achieve this, but instead it has been done by evaluating the difference between the Eurocode results and the ANSYS results for exactly the same configuration. This resulted in a correction factor which will be used in the calculation to determine the buckling load for different pad configurations in the next chapter.



Results

In this chapter the results of the different modelling configurations will be presented and discussed. Thereafter the relation between the results and the maintenance system are presented. For the different variables the tower and clamp model have been tested on buckling and yielding. The buckling load is defined as the loading condition for which buckling occurs first. The yielding is tested by looking at the von Mises criterion. The following results will be presented first: hardness, number of pads, width and height of the pad. By doing so a workable configuration can be presented for the investigated tower dimensions (with a diameter of 4 m and a thickness of 20 mm). The next step is to get more insight in the resistance of wind turbine towers of other dimensions (i.e diameter and wall thickness combinations). This is done in order to determine the loading capacity when the maintenance system is used for turbine towers of other dimensions.

For completeness the definition of loading capacity is given here: the loading capacity (L) is related to the maximum clamping force (F_{clamp}) that the tower can resist before being damaged. When the eccentricity is zero the loading capacity is: $L = \frac{F_{clamp}\mu_c}{g}$. This load consist of the clamp, crane and crane mass and is therefore given in metric tons. Furthermore; the clamping load can be translated into a clamping pressure (pressure exerted on the pads), when dividing the clamping force by the contact area of the clamp ($P_{clamp} = F_{clamp}/A$). A last note to keep in mind; in section 8.1, 8.2 and 8.3 the tower dimensions with which is worked are constant ($D=4m$ and $t=20mm$) and the load eccentricity is zero. In table 8.1 a list of symbols is given that will be used in this chapter.

Elastic Modulus	E	[Mpa]
Number of Pads	N	[-]
Width of Pad	W	[deg]
Height of Pad	H	[m]
Diameter Tower	D	[m]
Thickness Tower	t	[mm]
X-eccentricity	e	[m]
Gap between Pads	β	[deg]

Table 8.1: Legend

8.1. Elasticity

In this section the effect of the elastic modulus of the elastic layer is determined. There will exclusively be looked at the the von Mises stress, because we are interested in the stress distribution as a result of variable elasticity of the elastic layer. The investigation has been done for one specific case as was described in chapter 6.1.1 ($N=4$, $W=70$ deg, $D=4m$, $t=20mm$). First a visual inspection will be done and afterwards the maximum stress for varying material conditions will be presented quantitatively.

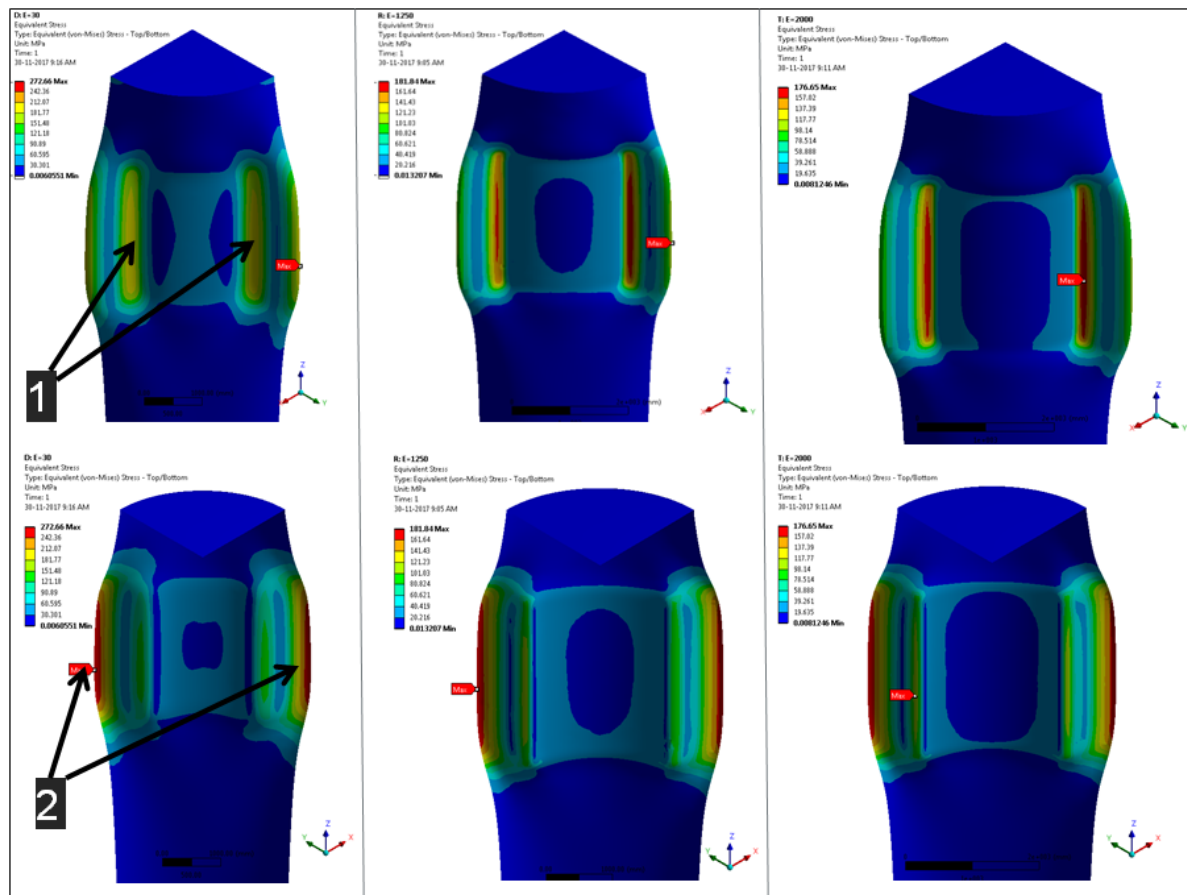


Figure 8.1: Von Mises stress on the outside (up) and inside (down) of the modelled tower section $E=30$ Mpa (left), $E=1250$ MPa (middle), $E=2000$ MPa (right)

In figure 8.1 the stress distribution on the tower section is given for an increasing Elastic Modulus. Here the results can be seen for an elastic modulus of 30, 1250 and 2000 Mpa. These specific cases have been selected, because a great variety in stress distribution can be observed.

Two locations have been identified where high stresses occur as identified in figure 8.1: on the edge of the pad (location 1) and in between the pads (location 2), which is the edge of the model in figure 8.1.

On the left figure the stresses are more equally distributed over the tower section and the stresses on the edge of the pad are not so high, but the peak stress on the edge of the model is highest of the three tests. For the second case, where $E=1250$ Mpa, a higher peak can be observed on the edge of the pad (location 1), but also here the maximum stress is observed on the edge of the tower section. On the third figure the maximum stress is observed on the edge of the pad. The maximum stress in between the pads is low. More generally can be said that the higher the E-modulus the more the stress is concentrated at the location where the pad touches the tower. A low elastic modulus has the opposite effect; the stress is distributed more equally on the edge of the pad and the peak is observed in between the pads.

When looking at figure 8.2 this same development can be observed. In this figure, blue indicates the configurations where the maximum stress is observed in between the pads (location 2) and red indicates the configurations where the maximum stress is observed on the edge of the pad (location 1). This figure also shows an increase in maximum stress for a lower E-modulus; a shift takes place from stress the edge of the pad to the location in between the pads. A second observation that is valuable for this investigation is that the maximum stress is not decreasing much when the E-modulus of the elastic layer is higher than thousand Mpa.

From these model tests three important observations were done: (1) a shift in location of maximum stress is observed depending on the Elastic modulus of the elastic layer, where for an more stiffer material, the peak stress will shift to the edge of the pad. The harder the material the more concentrated the stress will be on the edge of the pad. This is of importance for the selection of the material, because stress concentration

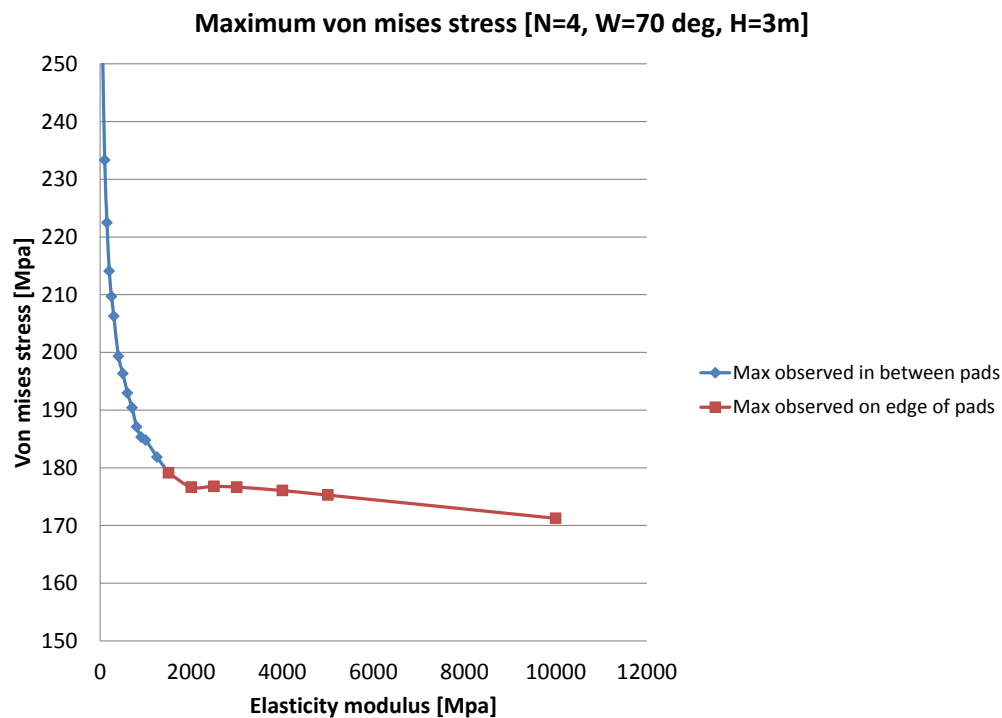


Figure 8.2: maximum von Mises stress for increasing flexibility of the elastic layer

can damage the tower structure. (2) For a hard material ($E > 1000$ Mpa), the peak stress is not decreasing considerably for a stiffer elastic layer. This means that for this configuration an E-modulus higher than thousand MPa is sufficient. From the figure it can be observed that the higher the E-modulus the lower the maximum observed stress and therefore it is favourable to select a material with a high elastic modulus. For application the material must not be too stiff, to avoid damage of the contact surface. Therefore

8.2. Number of Pads

In this section the maximum load for a variable number of pads will be looked at. It should be mentioned that the reducing the number of pads to a minimum is favourable when considering the complexity of the structure. However, the loading capacity of the tower structure is of major importance therefore here we focus on the effect of increasing the number of pads.

This will be done by analyzing the buckling and yielding results for the tested configurations. Although failure will occur when the lowest value is reached (yielding or buckling), both mechanisms follow a different trend and therefore it is interesting to look at them separately. There are different methods to analyze these results. First the effect of adding more pads will be evaluated, for a constant pad width. Secondly the focus is on cases where the gap between the pads (β) is kept constant.

8.2.1. Increase in number of pads for constant pad width

From table 8.2 it is observed that the yielding load is increasing when more pads are added. This quadratic looking trend is shown in figure 8.4 for a pad width of twenty degrees. In this figure the position of the maximum stress is located in between the pads. When the number of pads is increased the distance between the pads (indicated with β) is lowered and therefore the loading capacity increases.

The maximum stress in between the pads can be broken down in the hoop stress (that was defined in

Yield load [mt]				
Pad Width	N pads			
[deg]	3	4	8	12
20	21	23	134	360
40	29	37	574	x
60	37	91	x	x
70	43	171	x	x
80	55	361	x	x

Buckling load [mt]				
Pad Width	N pads			
[deg]	3	4	8	12
20	117	159	210	210
40	130	168	211	x
60	151	188	x	x
70	154	196	x	x
80	175	201	x	x

Table 8.2: Resulting buckling and yield loads for variable number of pads

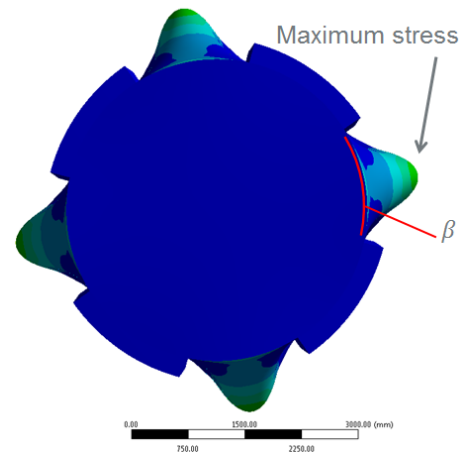


Figure 8.3: Deformation and stress results (55x enlarged) for N=4, W=40

section 7.2) and the bending stress. This bending stress is a result of the gap between the pads, because it is exactly here where the material 'bends' in radial direction as can be seen in figure 8.3. When the pad is widened the distance where the bending can occur is reduced and thereby reducing the bending stress. When the full circumference is enclosed there won't be a peak stress between the pads as a result of this bending stress; the maximum stress will be the result of the hoop stress alone. The bending stress is a large contributor to the stress in between the pads¹ and by decreasing the gap between the pads this effect is reduced. Now, when adding more pads, this distance β is reduced and therefore the yield capacity increases.

On the contrary the buckling load seems to be limited for increasing number of pads (figure 8.3). Here an asymptotic value is seen: when the number of pads increase the buckling load reaches a maximum value of 211. When the number of pads is higher than six, the buckling load reaches this limiting value.

The explanation for this maximum value can be found in the buckling load for a fully circumferential applied pressure: the buckling load that corresponds to this pressure correspond to the limiting buckling load. This means that when this upper limit is reached, adjusting the configuration of pads (adding more pads or widening them) doesn't influence the buckling load. Adjustments in that range, therefore are of minor importance. For the yielding load, the loading capacity can be increased considerably when increasing the number of pads. It was shown that by decreasing the gap between the pads, the loading capacity increases. This can be done by increasing the number of pads, but also by increasing the width of the pads. In this section we are interested in finding a favourable number of pads and therefore in the next part the results will be studied for configuration with variable number of pads, but a constant gap width.

8.2.2. Increase in number of pads for constant gap width

In this section the configurations presented in figure 8.5 will be looked at. In the search for the ideal number of pads the loading capacity of these four configurations will be compared. First the focus is on the results from the upper row, where β is fifty. The buckling load increases slightly when going from three to four pads. For the yielding load a small decrease is observed. When a selection between these two configurations should be made, the one with three pads is selected, because of the higher maximum loading capacity (of 43 mt). However, this load is far from the required loading capacity of 100 mt². To find loading capacities that can handle the required load, there will be looked at the configuration presented in the second line of figure 8.5. The gap is reduced (or in other words: the pads are widened) and thereby the yielding load is increasing from 37 mt to 358 mt and the yielding load is reaching its upper limit.

When comparing the lower row of figure 8.5, it shows that increase in number of pads has a slightly positive effect on the buckling load and the yield load. The buckling load goes from 201 mt to 210 mt and yielding load increases from 358 mt to 362 mt. The increase in load are small and when selecting a favourable config-

¹ Example: for the configuration presented in figure 8.3 the hoop stress is 26 times larger than the bending stress (σ_{hoop} 9 MPa and $\sigma_{bending}$ = 226 Mpa for maximum loading conditions)

² considering the 5 MW turbine

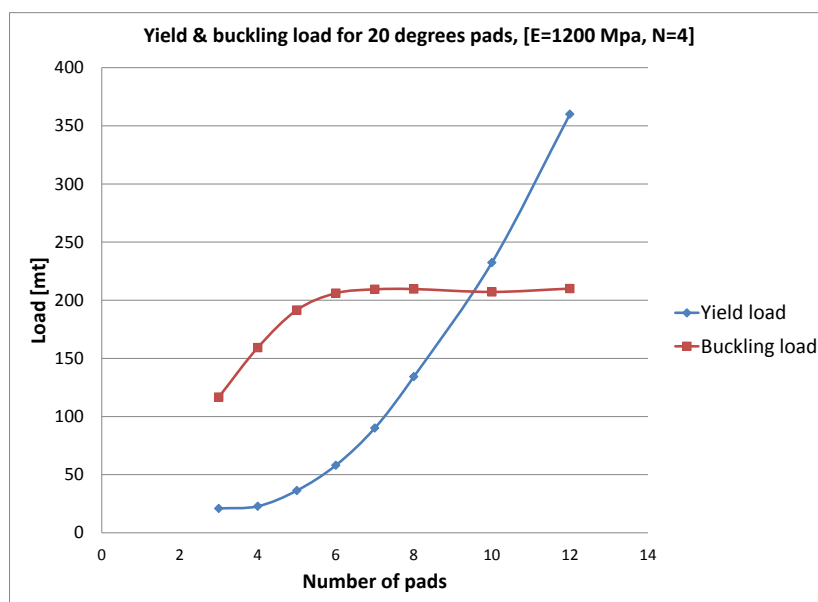


Figure 8.4: Buckling and yielding load for pad width $W=20$ degrees

uration also the complexity of the structure is considered.

From these observations it can be concluded: instead of increasing the number of pads widen them. Firstly because the complexity of the structure is increased and secondly because more loading capacity can be gained when widening the pad instead of increasing the number of pads (for a constant value of β).

Taken this into account in the next section a four pads setup is used and so keeping the number of pads to a minimum; the two pad setup is excluded because it will make opening of the clamp more difficult and three pad setup is unfavourable when the load on the clamp is eccentric.

8.3. Width and Height

In this section the results from varying the height and the width of the pad will be discussed simultaneously, because for both variables the area of the pad is increased and therefore it is interesting to evaluate and compare the effect on the loading capacity. This will be done first by looking at the maximum loading capacity for a centred load (eccentricity is zero) and after that the focus is on the effect of eccentricity. The latter can give valuable insight in the maximum loading capacity when the centre of gravity does not coincide with the center of tower structure, which is common in any lifting operation. At last possible configurations will be presented.

8.3.1. Centred Load

Also here there will be looked at buckling and yielding separately at first. The maximum pressure and maximum load are given³. First the buckling and then the yield results are discussed.

In figure 8.6b the maximum pressure is given for buckling. A negative trend can be seen; the maximum pressure is decreasing for increasing pad height. The effect of this negative trend on the loading capacity is shown in figure 8.7b. Here the loading capacity seems to converge to a maximum value when the pad height is increased. For the Eurocode calculation in section 7.3.1 the buckling load was independent of the height of the pressurized section when the slenderness reaches a specific value ($\lambda_p < \lambda_0$). This is not seen in figure 8.7b, but for increasing pad height and width of the pad setup the load converges to a maximum. The cases (eurocode and clamp setup) are not similar, because when the clamp is used only a segment of the

³the maximum pressure is defined as the pressure that is applied to the pads before failure occurs (buckling or yielding). The pressure can be translated to a clamping force using the pad surface. The load is calculated from this clamping force using the friction factor μ_c

Configuration	Buckling load [mt]	Yielding Load [mt]
1. N=3, W=70, $\beta=50$	154	43
2. N=4, W=40, $\beta=50$	168	37
3. N=4, W=80, $\beta=10$	201	358
4. N=5, W=62, $\beta=10$	210	362

Table 8.3: Resulting buckling and yielding load

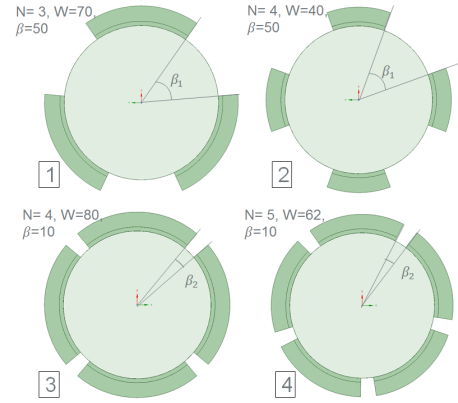


Figure 8.5: Top view of four configurations

tower section is loaded. Nevertheless, the increase in buckling load is small and can be a result of the pad configuration.

Another important observation from figure 8.7b: the influence on widening pad on the buckling load are small. For a pad height of 2 meter D1, D2 and D3 are respectively 25, 13 and 8 tons. These values even decreasing for an increase in pad height. An alternative to increase the loading capacity is to increase the pad height, but also here the increase in buckling load is limited, which is an important conclusion observing the buckling load. The next step is to focus on the second failure mode: yielding. In figure 8.6a an almost linear trend can be observed for increasing pad height. Here only a slight decrease in pressure is seen for a pad height of 2-4 meters, for longer pads these edge effects disappear and the pressure increases linear with the pad height. In figure 8.7a the pressure is translated into yielding load which results in the linear trend. Furthermore, in contrary to the buckling load the yield load can be increased considerably when increasing width or the height of the pad. This means that when yielding is the dominant failure mechanism, the loading capacity can be increased easily by widening or lengthening the pad.

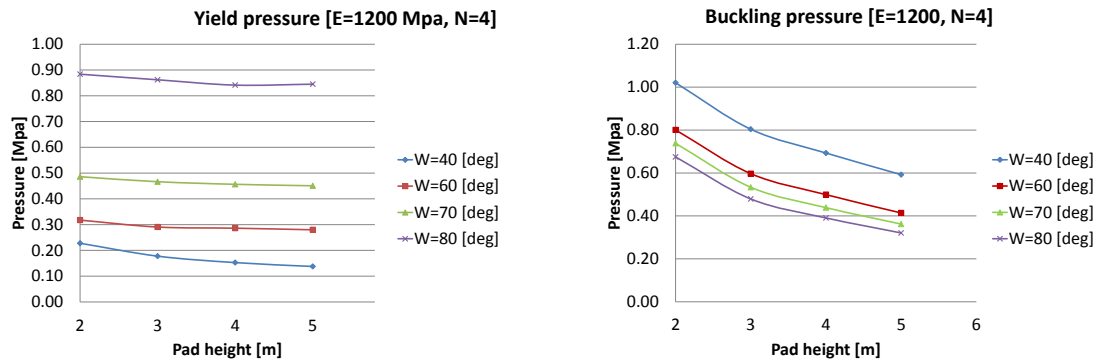
Now both failure mechanism where discussed separately those results should be combined; the lowest value, buckling or yielding, determines the loading capacity of the tower structure when a specific pad configuration is used. The results are presented in figure 8.8. The shaded area indicates the required loading capacity of hundred tons (for a 5 MW turbine) and not all configurations meet this requirement; the configuration with a pad width of forty and sixty degrees are (partly) in this shaded area. This figure also shows a shift in failure mechanism; from yielding to buckling. The squared marker indicates buckling failure. So for a pad width of 80 degrees, buckling is the prevailing failure mechanism and also for a pad width of seventy degrees with a pad height of minimum four meters. This shift in failure mechanism has implications for the design choices: when the tower failure mechanism is buckling, increasing width or height of the pad has limited impact on increasing the loading capacity. These observations where done for a centred load, in the next section the influence of an eccentric load will be included.

8.3.2. Eccentricity

For a centred load the tower only has to resist the clamping force that is needed to generate enough friction. For an eccentric load, also a moment is introduced (as described in section 5.2 and therefore the loading capacity is decreasing. In this section the effect of the load eccentricity is investigated. This will be done by first looking at the trends for yielding and buckling for a one configuration and secondly the loading capacity of four cases are presented that meet the requirements for a five megawatt turbine (100 tons at 8 meters).

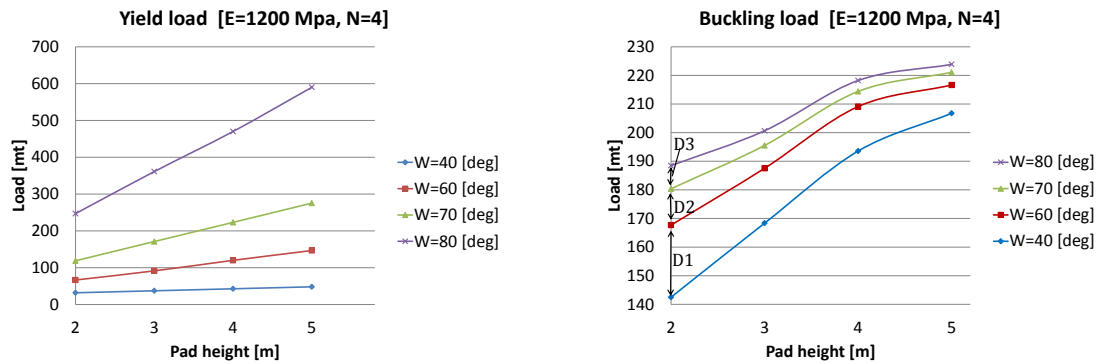
In figure 8.9 the yield and buckling load are shown for a specific case that meets the requirements ($E=1200$, $N=4$, $W=80$ deg and $H=3$). Looking at the trends separately will help to get a better understanding of both failure mechanisms and so adjustments for improvement can be done based on this failure mechanism⁴. For increasing load eccentricity, a steep decrease in yield load is observed and the buckling follows more gradually. This difference in shape can best be explained when looking at the forces that work on the tower structure when a moment is applied in figure 5.6. As a result of the moment force, the peak forces increase and thus the stresses increase at the positions where the peak forces are highest. The higher stresses result

⁴ For example when the tower fails by yielding, increase in pad high or width will help to increase the loading capacity.



(a) maximum yield pressure for centred load (e=0) (b) maximum buckling pressure for a centred load (e=0)

Figure 8.6: Yield and buckling pressure



(a) maximum yielding load [mt] (e=0) (b) Maximum buckling load [mt] (e=0)

Figure 8.7: Yield and buckling load

in a decrease in yield load. For buckling, it is not the peak stress but the total load that is exerted on the tower structure that influences the buckling load and therefore the decrease is less pronounced when load eccentricity is introduced.

When looking at the maximum load for this specific configuration the load capacity goes from 201 mt (e=0) to 136 mt (for e=8m). This decrease in loading capacity has to be taken into account in the search for the right pad configuration. However, this specific setup meets the requirements and therefore a workable solution is found. In figure 8.10 setups which meet these requirements are shown. When inspecting the load capacity for increasing eccentricity two pattern can be observed: (1) the blue line drops quickly for an increase in eccentricity and where yielding is the prevailing failing mechanism and (2) the gradually reducing load capacity for the other three configurations. Here buckling is the prevailing failure mode. In table 8.4 the loading capacity for these configurations is listed. The second configuration which was mentioned (Width = 80 deg, Height = 3m) has an acceptable height and assures a tower loading capacity of 136 mt for maximum eccentricity of four. This loading capacity is sufficient and therefore in the next section, where the influence of tower diameter and thickness is investigated this configuration will be used.

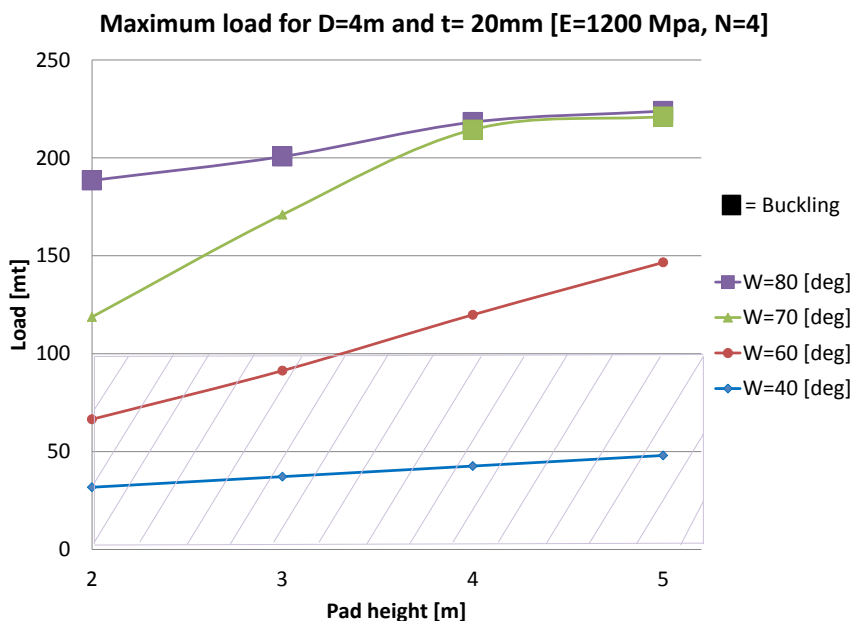


Figure 8.8: Maximum load for different pad configurations ($e=0$)

Load capacity for D=4m, t=20mm, e=8m	[mt]
1. E=1200 Mpa, N=4, W=70 deg H=5m	124
2. E=1200 Mpa, N=4, W=80 deg H=3m	136
3. E=1200 Mpa, N=4, W=80 deg H=4m	162
4. E=1200 Mpa, N=4, W=80 deg H=5m	185

Table 8.4: Configurations that meet the load and eccentricity requirements

8.4. Tower Diameter and Thickness

In the previous section a solution for the pad width and height was found. This solution was specifically found for a tower dimension $D=4$ and $t=20$ mm. In this section the resulting capacity for towers of variable diameter and thickness are presented. This will be done in two steps: (1) first the loading capacity for the investigated towers is visualized for zero eccentricity and then the some important loading capacities are presented⁵.

In figure 8.11 the loading capacity is given for zero load eccentricity. This shows the increase of the loading capacity for increasing thickness and diameter. Furthermore the shift from yielding to buckling is clearly visible. Each point on these graph indicate the loading capacity for a specific tower diameter and thickness for a centred load. However, for the applicability of the clamp the eccentricity should be introduced. This was done for all cases mentioned in section 6.1.4. In table 8.5 some important results for a load eccentricity of 8 meters are shown. These results look promising for the applicability of the maintenance system on a wide range of wind turbine towers⁶: for the configuration $D=3$ m $t=16$ mm (expected dimensions for a 4MW turbine) the loading capacity of 111 mt and thereby is sufficient for a gearbox replacement for a five megawatt turbine. When looking at the other end of the spectrum; for the configuration $D=6$ m, $t=22$ the loading capacity is 137 mt. This means that the tower has sufficient loading capacity for a gearbox replacement of a 6MW turbine.

In appendix E.3 the tower loading capacity is given for a load eccentricity of 0-8 meters and therefore can be used as a useful reference when using the clamping mechanism on a wind turbine tower.

⁵A complete overview of the results is presented in appendix E.3

⁶the total required loading capacity for gearbox replacement are 100, 130 and 160 mt for respectively a 5, 6 and 7 MW turbine.

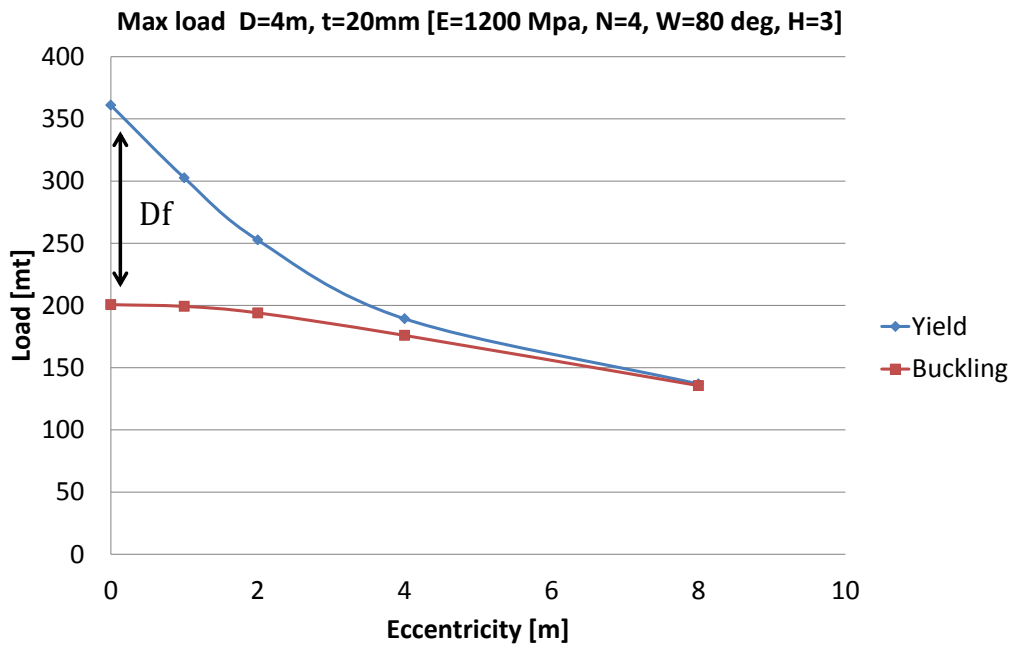


Figure 8.9: Yield and buckling load for increasing eccentricity

Maximum loading capacity for e=8m								
	D=3m		D=4m		D=5m		D=6m	
t[mm]	Load [mt]	t[mm]	Load [mt]	t [mm]	Load [mt]	t [mm]	Load [mt]	
16	111	18	90	20	115	22	137	
18	155	20	135	22	158	24	179	
20	201	22	179	24	201	26	222	

Table 8.5: Loading capacity for [E=1200 Mpa, N=4, W=80 deg, H=3m]

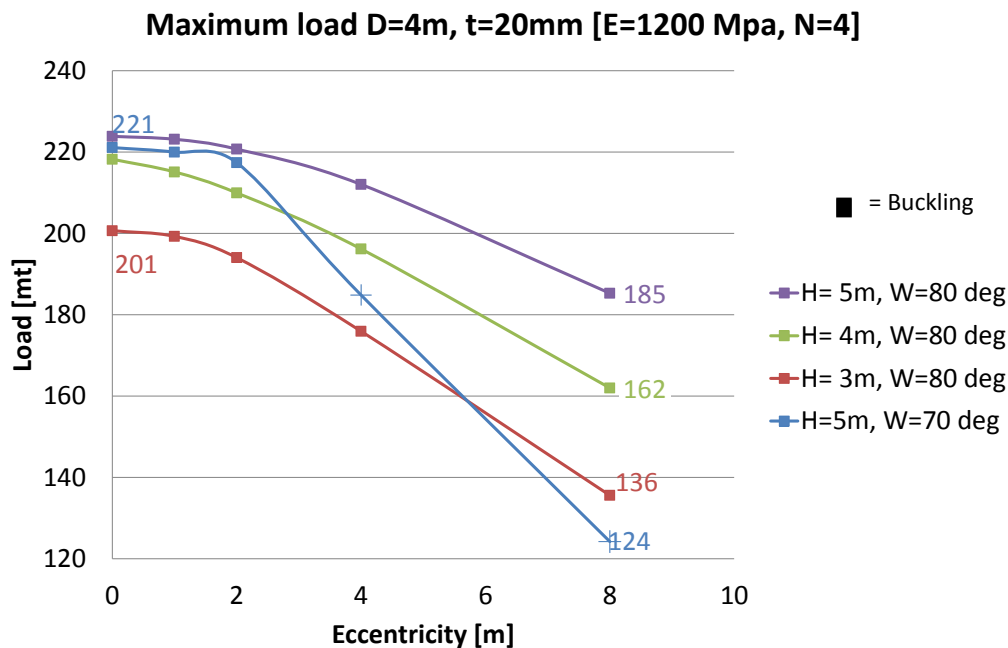


Figure 8.10: Maximum load for increasing eccentricity

8.5. Conclusions

In this chapter we looked at the elasticity, number of pads, width and height of the pad. When looking at the elasticity of the material it was seen that material should not be too soft, because this will result in high stresses in between the pad, but also not too hard, because then the maximum stress will concentrate on the edge of the pad. The elastic modulus was varied from 10-10000 Mpa and it was observed that the stress was not decreasing considerably when higher E-modulus than 1000 was used. Therefore the selected material will have an E-modulus of 1200 Mpa.

When looking at the number of pads it was observed that the increase in number of pads has a positive influence on the maximum observed stress in the tower. However, a trade-off has to be made between the complexity of the structure and the increase in loading capacity for increasing number of pads. What also can be done to increase the loading capacity is widen the pad. By doing so the complexity of the structure can be minimized and therefore in the further investigation it was chosen to use a configuration of four pads.

The width and height have also been considered and it was seen that the buckling stress is the dominant failure criterion for a wide pad ($W \geq 80$ [deg]). Looking at the yielding load it was observed that the stress reduction is large for increasing pad width. However, for $W \geq 80$ [deg] the dominant failure criterion is buckling. When this is the failure criterion, increasing the width of the pad does increase the loading capacity. However these changes are small (for increasing the width from 70 to 80 degrees, the maximum loading capacity increases less than 5%). In short: when selecting the right width of the pad, the maximum loading capacity can be increased considerably until buckling is the prevailing failure mechanism, therefore the favourable pad width is 80 degrees.

When looking at the length of the pad a similar pattern was observed; the maximum load increases linearly with increasing length of the pad when looking at yielding. However, the buckling load is increasing slightly for increasing pad height (conform the used Eurocode where the buckling load is constant for increasing length). When selecting the right pad height the maximum loading capacity can be increased when the structure fails by yielding. In short: the maximum loading capacity is a combination of width and height of the pad and can be increased considerably until buckling is the prevailing failure mechanism. This brings

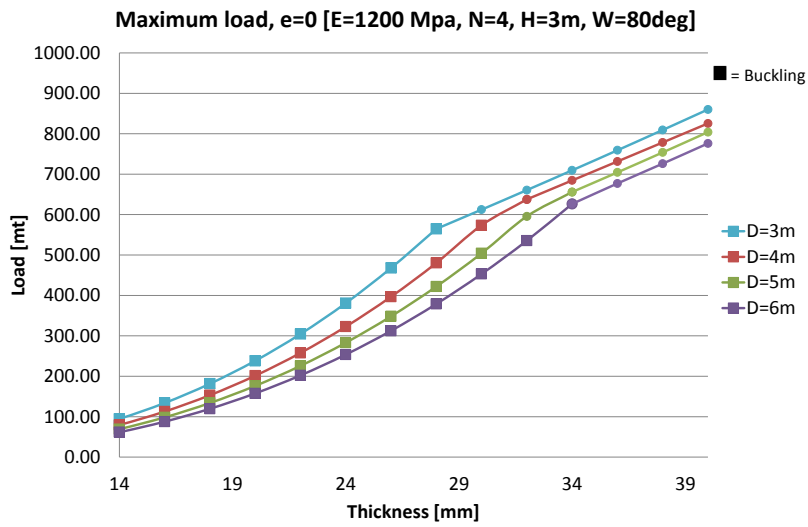


Figure 8.11: Maximum centred load for increasing tower thickness

us to the selected configuration (for tower diameter of 4m and thickness of 20mm): number of pads is 4, pad width is 80 degrees, pad height is three meters.

The load capacity for towers of variable diameter and thickness were presented in the last section and here it was shown that the configuration is applicable on a wide range of wind turbine towers.

9

Conclusions and Recommendations

9.1. conclusions

The demand for affordable renewable energy has put pressure to cost reduction in the offshore wind market. Operation and maintenance costs of offshore wind turbines are high, therefore alternative methods should be developed to reduce these costs. The replacement of heavy components, like a gearbox or a generator, is a frequently occurring operation that can be improved. This was used as a starting point for this research.

Current developments are addressing the problem of reducing the maintenance costs, but still two important downsides are present: (1) insufficient lifting capacity for gearbox replacement and (2) most systems are designed to be used on specific turbines. Nevertheless these concepts gave valuable information on techniques that can be used for maintenance purposes; the Anson and Vestas crane smartly use the tower structure to install their maintenance system.

Before using this knowledge to generate concepts, a thorough inspection of the offshore wind turbine tower and gearbox was done. Although turbines vary greatly, the tower and nacelle frame were identified as strong connection points for a maintenance system. Furthermore, the weight of the gearbox has been investigated, showing a linear trend between the gearbox weight and the size of the turbine can be observed. This is valuable information when designing a maintenance system that should work on a range of wind turbines.

The investigation of available maintenance systems, has provided a firm base to generate concepts. This resulted in four concepts: (1) the climbing crane, (2) self-lifting crane with clamp, (3) base attached tower and the (4) pulley lifting method. Evaluation of these concepts has resulted in the selection of the most promising concept; the self-lifting crane with clamp. This solution consists of a small crane which is installed on the wind turbine tower from a floating vessel. A great advantage over currently used method is that no specialized maintenance vessel is required for a gearbox replacement and thereby costs and time can be saved.

The crane is attached to the tower structure by the use of a clamping mechanism and it remains its position by generating frictional force. To generate this force, hydraulic cylinders are pressing the pads against the tower structure. For the applicability of this concept it is of major importance that the structural integrity of the tower is maintained, while sufficient frictional force is generated to avoid the crane from slipping down during lifting operations. Therefore, in the second part of this thesis a feasibility study was done on the application of this clamping mechanism on wind turbine towers. To be more specific: the goal was to find a contact surface configuration such that the crane and its load remain their position and the structural integrity of the tower is assured.

This was done in three steps: (1) defining the clamp and identifying variables of interest, (2) translate this into FEM model setup and (3) analyze and interpret the results. First a preliminary design of the clamp and its working principle was presented and the loads were determined: for a five megawatt turbine the wind turbine tower should be able to resist a load of hundred tons at 8 meter (130 tons for a 6MW turbine and 160 tons for a 7MW turbine). Thereafter, the variables of interest were defined: (1) elasticity of the contact layer, (2) number of pads used, (3) width and (4) height of the pads. The latter three relate to the contact surface area and the elasticity of the contact layer influences the distribution of the forces from the clamp to the tower structure.

Secondly, using ANSYS workbench the variables have been translated into a finite element model. A combination of shell and solid elements has been used to build an efficient model of the pads and the wind turbine tower.

Finally the results were analyzed. The high load requirements influence the dimensions of the clamp structure. Nevertheless, the results showed possibilities to meet the requirements. It can be concluded that; the proposed solution should have a contact layer where the elasticity modulus (E) is higher than 1200 Mpa. By adding more pads, the loading capacity increases. However, it also results in a more complex structure and therefore it is advised to reduce the number of pads (N) and instead widen them. Considering this trade off, a four pad configuration was selected to determine the required width (W) and height (H) of the pads. For the four pad setup a pad width of eighty degrees and pad height of three meter is used to meet the requirements of replacing the gearbox, the heaviest component of the wind turbine powertrain. For this specific configuration (i.e. $E=1200$ Mpa, $N=4$, $W=80$ deg, $H=3$), the loading capacity of a wind turbine tower is 138 tons for an eccentricity of eight meters ¹.

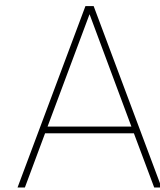
Furthermore, to assure this clamping mechanism works on towers of different dimensions (i.e. diameter and wall thickness combinations), the loading capacity was determined for a variety of tower dimensions. Insights have been gathered on the application of this clamping mechanism on different turbines. To make the data useful for further application, tables are included which indicate the loading capacity for towers with a diameter of three to six meters (see appendix E).

9.2. Recommendations

To assure optimal performance of the proposed system, further investigation has to be conducted:

- The clamp and the tower structure were modeled as a perfect connection. In reality the tower might not be perfectly round. It is advisable to check till what extent this shape can deviate. Furthermore; welding seams can be present on the location where the clamp is installed. Although safety factors have been used to account for material inconsistencies, installing the clamp on a welding seam can cause hazardous situations. Investigation of the loading possibilities of these seams is therefore required.
- The rubber layer was simulated as a solid element, whereas in industry blocks or strips are used. In this configuration there is space for the material to extend. However, not the whole contact surface will be covered and this can influence the load distribution on the tower structure.
- In the ANSYS model a rubber layer with a thickness of 110 millimeters was used. The required elasticity of this layer is based on this thickness. Adjusting the thickness will influence its performance. For a thinner layer the stresses on the edge of the pads will increase and thus the material properties should be adjusted to compensate for this change.
- A static analysis was done on the clamp tower configuration, thereby neglecting the dynamic process of a lifting operation.
- While determining the loading capacity only the load eccentricity in one direction has been taken into account. The eccentricity in the second direction has been neglected. The eccentricity of 8 meters in one direction is an extreme loading case, however the load eccentricity in the second direction should also be checked.
- The applied load on the pad was equally distributed. In reality hydraulic cylinders are pushing the pads against the tower structure and the load distribution depends on the positioning of these connections. This effect should also be investigated.

¹ this is the loading capacity based on a tower diameter of 2 meter and wall thickness of 20 millimetre



Turbine data

Type	Power rating [MW]	Weight [mt]	Length [m]	Source
Vestas V90-3MW	3	23	-	sparesinmotion.com
Vestas V80 2MW	2	14.5	-	sparesinmotion.com
Gamesa G87 2MW	2	15.8	-	sparesinmotion.com
AD 180 8MW	8	86	-	sparesinmotion.com
Gearbox 2.5 MW	2.5	19.5	-	sparesinmotion.com
Gearbox 2.2 MW	2.2	16.4	-	sparesinmotion.com
Gearbox 0.75 MW	0.75	4.3	-	sparesinmotion.com
Gearbox 0.66 MW	0.66	3.2	-	sparesinmotion.com
Gearbox 3.0 MW pph (rotor side integrated)	3	23	2.8	zf.com
Gearbox 4.5 MW pp (rotor side integrated)	4.5	70	6	zf.com
pph (generator side integr)	6.15	63	4	zf.com
pph (generator side integr)	3.6	30	3.7	zf.com
pph (generator side integr)	3	28.85		zf.com
phh (generator side integr)	2.05	19		zf.com
phh (generator side integr)	2	15	2.2	zf.com
phh (generator side integr)	2	15	2.7	zf.com
differential design	8	70	3	zf.com

Table A.1: Gearbox data

Height of transition piece (TP)					
Wind Farm	TP (above MSL) [m]	depth [m]	Foundation type	Power	source
BELWIND	17	15-37	monopile	3 MW	Huisman
Alpha Ventus (Ger)	15	30	Tripod/jacket	5 MW	Huisman
Beatrice	19	45	tripod	5 MW	Huisman
Hoeksiel	19	45	tripod	5 MW	Huisman
Horns Rev	9	6-14	monopile	2 MW	Huisman
Horns Rev 2	13	11-14	monopile	2.3 MW	Huisman
Kentish	8	5	monopile	3 MW	Huisman
Prografica	3.5	6-10	gravity	2.3MW	Huisman
Rodsand	3.5	6-12	gravity	2.3MW	Huisman
Burbo Bank	22	4-17	monopile	8 MW	4coffshore.com
Gunfleet sand	18	0-13	monopile	3.6MW	4coffshore.com
Owez	13	15-18	monopile	3MW	4coffshore.com
Lynn/inner Dowsing	21	6-14	monopile	3.6MW	4coffshore.com
Rhyl Flats	23	6-12	monopiles	3.6MW	4coffshore.com
Robin Rig	20	4-13	monopile	3MW	4coffshore.com

Table A.2: Height transition piece for wind turbine parks on the North Sea

B

FEM introduction

The FEM principle: the equations to describe the distribution of stresses are known, but they cannot be directly solved for a complicated shape. However these equations can be solved for simple shapes like triangles or rectangles. FEM takes advantage of this fact and divides the complete structure in these simple elements (the Finite Element Mesh). These elements are defined by nodes and at these nodes the behaviour is described by a set of simultaneous algebraic equations :

$$Ku = f \tag{B.1}$$

In this research there is looked at a structural problem and therefore the behaviour at a node can simply be described as a system with a spring where the properties of the material are presented in the stiffness matrix K , the behaviour of the node is given as in the displacement vector \mathbf{u} and the action is represented by the force vector f . From equation (B.1) it can be seen that f presents the external energy or work. When we want to know the properties of a structure, for each element fifteen equations (among which 9 are partial differential equations) need to be solved for each material point (or node):

Equilibrium equations (3)

Strain-displacement relations (6)

Stress-strain relations (Hooke's law) (6)

In short: (1) FEM is solving the set of algebraic equation for every node, (2) uses the concept of piece-wise polynomial interpolation and (3) connects all the elements together, such that the field quantity becomes interpolated over the entire structure node after node.

As any other research is it of great importance to inspect the performance of the simulations. Also The results should also be inspected on reliability, just as accuracy of the results. FEM simulations can be time consuming and therefore a balance between acceptable precision and time consuming simulations should be found. To assure reliability and precision we follow the cycle of analysis given by Lee [9] (2010, p.282):

1. **Pre-processing:** (discretization domain, derive equations and assemble/combine equations) Important here is to define the element type and the mesh configuration
2. **Solution:** here a distinction needs to be made between a linear problem and a non-linear problem. The first can be performed without difficulties; the quality depends on the FEM method itself. The non-linear problem has to be solved iteratively and a solution can only be found if convergence occurs. Here the settings for when convergence is achieved effects the accuracy of the results. In the figure we can see the Newton Raphson iteration scheme.
3. **Post processing:** interpreting the results.

B.1. Pre-processing

Elements and mesh need to be determined in this part. There are three types of elements that can be chosen; (1) beam, (2) shell and (3) solid elements. In this research a combination of shell and solid elements will be used.

Element shape: *include here*

Mesh refinement: the size of the elements should be such that all the details of the displacements are covered, but a difference should be made between parts where high gradients of displacement/stresses occur. There a finer mesh is required to cover the changes in displacement/stresses. In our research we select the specific areas where the displacement/stress gradients are high and increase the number of elements on these specific places. By doing so the computational time is reduced in comparison by increasing the number of elements for the complete structure. An example can be seen in figure ???. In this figure we see a pile where the mesh is around the location where the force works on the structure. Even with the right meshing irregularities can occur and therefore we check the results on smoothness and aspect ratio. The smoothness is the change in size of the elements. With a sudden change in size stress and displacement can be visualized inaccurately. The aspect ratio is the ratio between the longest and shortest side of an element. We will get the best results when the ratio is 1 for multidimensional flow.

Boundary conditions: defining the boundaries of a model is of importance, since finding a solution with FEM often is solving a boundary value problem. The selection of the boundary conditions influences the results and obviously should be chosen with care. Keeping a structure and its boundary conditions as simple as possible is one of the most important general rules using FEM. In this research this has been chosen as starting point. A division between two types of BC can be made; (1) essential and natural boundary conditions. The first influences the DOF directly and can be found on the left side of the equilibrium equation in the u vector. Natural boundary conditions, on the other hand, do not influence the DOF directly and can be found on the right side of the equilibrium equations, like forces.

B.2. Solution

The linear buckling analysis done in ANSYS consist of the following steps: (1) a load is applied to the structure which is used as a reference. Then a linear static analysis is carried out to obtain stresses that are needed to form the geometric stiffness matrix K_g . Then the buckling load can be calculated as part of the second load step, by solving the eigenvalue problem:

$$(K - \lambda K_g)x = 0 \quad (\text{B.2})$$

Where K is the stiffness matrix of the structure and λ is the multiplier of the reference load. x represents the eigenvector which correspond to the eigenvalue. ANSYS uses the Lanczos method to solve this eigenvalue problem (see for example Rajakumar and C. and Rogers [12]). Since the lowest eigenvalue is associated to buckling, only the first eigenvalue will be calculated. The buckling load will be given as:

$$F_{crit} = \lambda_{ult} F_{ref} \quad (\text{B.3})$$

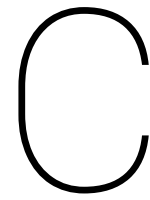
In our case the multiplier λ will be the unknown such that

$$\lambda_{ult} = F_{crit} / F_{ref} \quad (\text{B.4})$$

The F_{ref} is given as the load that is applied on the tower by the clamp and λ_{ult} is the result given by ANSYS.

B.3. Post-Processing

The last step is to analyze and interpret the results and the goal here is to assure the right modelling procedure is followed. Here the model should be checked on irregularities and improved where necessary. Stresses and displacements should change gradually increase/decrease and visual inspection is a tool to do so. Besides inspecting the stress distribution of a system, in ANSYS workbench a method to find irregularities is the energy error approach. This basic idea of this method is that the difference between the average stress and the interpolated stress at a node is used to calculate the energy error of the structure. It can easily be understood that when the mesh is very coarse, the energy error will increase. When using this method, location that where mesh refinement is needed can easily be located. When the post-processing is done and the results are not satisfying, the model should be improved.



Hoop stress comparison

N	4								
W	70	deg							
P	0.2	Mpa							
D=3m				D=4m			D=5m		
t [mm]	Analytical	ANSYS	delta	Analytical	ANSYS	delta	Analytical	ANSYS	delta
9	27	35	8	x	x	x	x	x	x
11	22	28	6	29	33	4	x	x	x
13	19	24	5	25	29	4	x	x	x
15	16	21	5	22	26	4	27	32	5
17	14	19	4	19	23	4	24	27	3
19	13	17	4	17	20	3	21	23	2
20	12	16	4	16	19	3	20	22	2
22	11	14	3	15	18	3	18	20	2
24	10	13	3	14	16	3	17	19	2
26	9	12	3	12	15	3	16	18	2
28	9	11	3	12	14	2	14	16	2
30	8	11	3	11	13	2	14	15	2
32	8	10	2	10	12	2	13	14	2
34	7	9	2	10	12	2	12	14	2
36	7	9	2	9	11	2	11	13	2
38	6	8	2	9	10	2	11	12	1
40	6	8	2	8	10	2	10	12	1
45	5	7	2	7	9	2	9	10	1
50	5	6	2	6	8	1	8	9	1

Table C.1: Hoop stress [Mpa] comparison analytical and ANSYS results

D

Offshore Wind Turbine

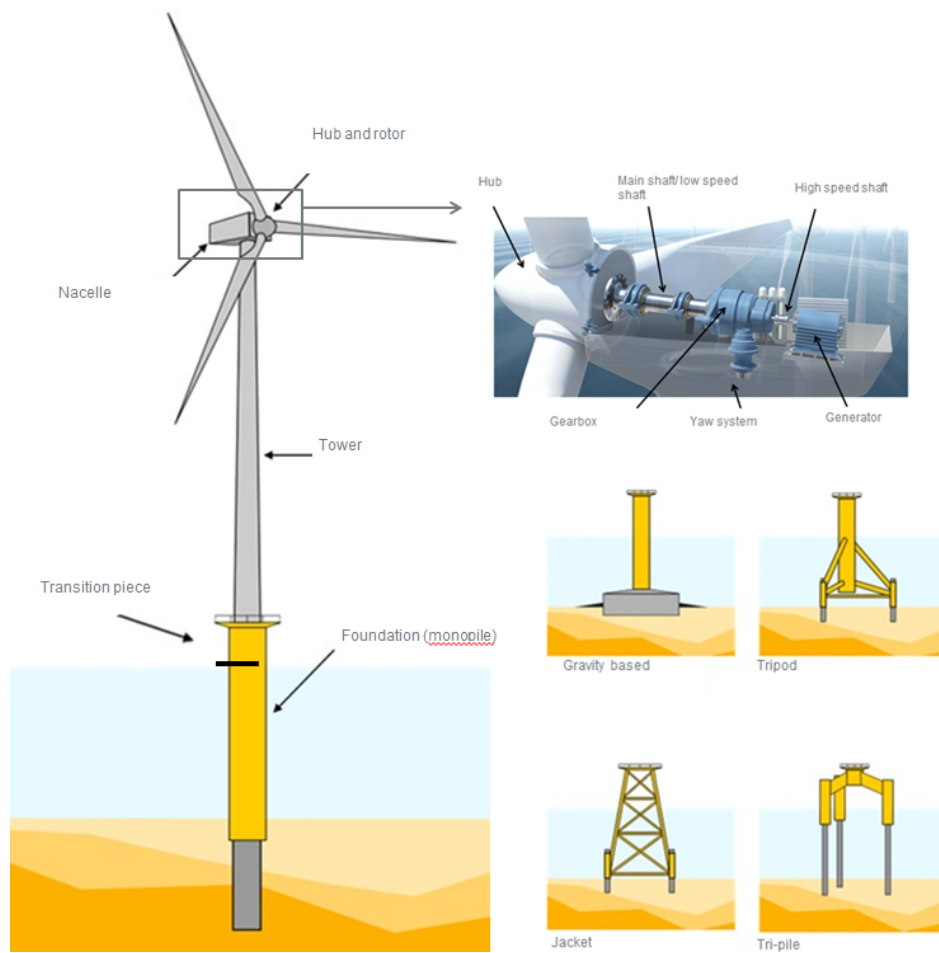


Figure D.1: Offshore Wind Turbine

E

Tables

E.1. Pad Height and Width

Clamping Capacity Wind Turbine Tower [kN]						
Pad Width		Pad Height [m]				
[m]	[deg]	2	3	4	5	
1.4	40	3179	3720	4261	4802	
2.1	60	6650	9131	11985	14658	
2.4	70	11874	17097	21440	22108	
2.8	80	18846	20066	21822	22385	

Loading Capacity Wind Turbine Tower [mt]						
Pad Width		Pad Height [m]				
[m]	[deg]	2	3	4	5	
1.4	40	32	37	43	48	
2.1	60	66	91	120	147	
2.4	70	119	171	214	221	
2.8	80	188	201	218	224	

Conditions		
Rubber Elasticity	1200	[-]
Number of Pads	4	[m]
Width of pad	40-80	[deg]
Height of pad	2-5	[m]
Diameter Tower	4	[m]
Thickness Tower	20	[mm]
Eccentricity	0	[m]
Yield Strength	355	[Mpa]
Rubber Thickness	110	[mm]
Rubber Elasticity	1200	[Mpa]
Friction Coefficient	0.15	[-]
sf yield	1.5	[-]
sf buckling	1.5	[-]
sf friction	1.5	[-]

Legend	
Buckling failure	
Yielding failure	

Yielding		Clamping Capacity Wind Turbine Tower [kN]				
Pad Width		Pad Height [m]				
[m]	[deg]	2	3	4	5	
1.4	40	3179	3720	4261	4802	
2.1	60	6650	9131	11985	14658	
2.4	70	11874	17097	22305	27534	
2.8	80	24679	36109	46990	58990	

Yielding		Loading Capacity Wind Turbine Tower [mt]				
Pad Width		Pad Height [m]				
[m]	[deg]	2	3	4	5	
1.4	40	32	37	43	48	
2.1	60	66	91	120	147	
2.4	70	119	171	223	275	
2.8	80	247	361	470	590	

Buckling		Clamping Capacity Wind Turbine Tower [kN]				
Pad Width		Pad Height [m]				
[m]	[deg]	2	3	4	5	
1.4	40	14249	16836	19356	20676	
2.1	60	16769	18753	20910	21664	
2.4	70	18039	19552	21440	22108	
2.8	80	18846	20066	21822	22385	

Buckling		Loading Capacity Wind Turbine Tower [mt]				
Pad Width		Pad Height [m]				
[m]	[deg]	2	3	4	5	
1.4	40	142	168	194	207	
2.1	60	168	188	209	217	
2.4	70	180	196	214	221	
2.8	80	188	201	218	224	

Loading Capacity Wind Turbine Tower [mt]					
Pad Width		Pad Height [m]			
Width [deg]	eccentricity [m]	2	3	4	5
60	0	67	91	120	146
60	1	58	80	105	128
60	2	50	70	93	114
60	4	40	56	75	93
60	8	28	40	54	68
W	e	2	3	4	5
70	0	119	171	214	221
70	1	105	151	202	220
70	2	88	133	180	217
70	4	64	100	140	185
70	8	42	62	88	124
W	e	2	3	4	5
80	0	188	201	218	224
80	1	184	199	215	223
80	2	161	194	210	221
80	4	117	176	196	212
80	8	68	136	162	185

Conditions		
Rubber Elasticity	1200	[Mpa]
Number of Pads	4	[-]
Width of pad	60-80	[deg]
Height of pad	2-5	[m]
Diameter Tower	4	[m]
Thickness Tower	20	[mm]
Eccentricity	0-8	[m]
Yield Strength	355	[Mpa]
Rubber Thickness	110	[mm]
Rubber Elasticity	1200	[Mpa]
Friction Coefficient	0.15	[-]
sf yield	1.5	[-]
sf buckling	1.5	[-]
sf friction	1.5	[-]

Legend
Buckling failure
Yielding failure

Buckling						
Loading Capacity Wind Turbine Tower [mt]						
Pad Width		Pad Height [m]				
Width [deg]	eccentricity [m]	2	3	4	5	
60	0	168	188	209	217	
60	1	163	186	205	216	
60	2	150	179	200	213	
60	4	120	155	183	202	
60	8	82	114	143	170	
W	e	2	3	4	5	
70	0	180	196	214	221	
70	1	175	194	211	220	
70	2	164	188	205	217	
70	4	134	167	190	208	
70	8	92	125	152	178	
W	e	2	3	4	5	
80	0	188	201	218	224	
80	1	184	199	215	223	
80	2	174	194	210	221	
80	4	147	176	196	212	
80	8	103	136	162	185	

Yielding						
Loading Capacity Wind Turbine Tower [mt]						
Pad Width		Pad Height [m]				
Width [deg]	eccentricity [m]	2	3	4	5	
60	0	67	91	120	146	
60	1	58	80	105	128	
60	2	50	70	93	114	
60	4	40	56	75	93	
60	8	28	40	54	68	
W	e	2	3	4	5	
70	0	119	171	223	275	
70	1	105	151	202	255	
70	2	88	133	180	231	
70	4	64	100	140	185	
70	8	42	62	88	124	
W	e	2	3	4	5	
80	0	247	361	471	590	
80	1	198	303	422	546	
80	2	161	253	359	475	
80	4	117	189	276	373	
80	8	68	137	168	228	

E.2. Number of Pads

Clamping Capacity Wind Turbine Tower [kN]						
Pad Width		Number of pads				
[m]	[deg]	3	4	8	12	
0.7	20	2099	2285	13429	36030	
1.4	40	2890	3720	57359	x	
2.1	60	3663	9131	x	x	
2.4	70	4260	17097	x	x	
2.8	80	5521	36109	x	x	

Loading Capacity Wind Turbine Tower [mt]						
Pad Width		Number of pads				
[m]	[deg]	3	4	8	12	
0.7	20	21	23	134	360	
1.4	40	29	37	574	x	
2.1	60	37	91	x	x	
2.4	70	43	171	x	x	
2.8	80	55	361	x	x	

Clamping Capacity Wind Turbine Tower [kN]										
Pad Width		Number of pads								
[m]	[deg]	3	4	5	6	7	8	10	12	
0.7	20	2099	2285	3631	5806	9012	13429	20716	21002	

Loading Capacity Wind Turbine Tower [mt]										
Pad Width		Number of pads								
[m]	[deg]	3	4	5	6	7	8	10	12	
0.7	20	21	23	36	58	90	134	207	210	

Conditions		
Rubber Elasticity	1200	[Mpa]
Number of Pads	3-12	[-]
Width of pad	20-80	[deg]
Height of pad	3	[m]
Diameter Tower	4	[m]
Thickness Tower	20	[mm]
Eccentricity	0	[m]
Yield Strength	355	[Mpa]
Rubber Thickness	110	[mm]
Rubber Elasticity	1200	[Mpa]
Friction Coefficient	0.15	[-]
sf yield	1.5	[-]
sf buckling	1.5	[-]
sf friction	1.5	[-]

Legend	
Buckling failure	
Yielding failure	

!

Yielding						
Clamping Capacity Wind Turbine Tower [kN]						
Pad Width		Number of pads				
[m]	[deg]	3	4	8	12	
1.4	20	2099	2285	13429	36030	
	40	2890	3720	57359	x	
2.1	60	3663	9131	x	x	
2.4	70	4260	17097	x	x	
2.8	80	5521	36109	x	x	

Yielding						
Loading Capacity Wind Turbine Tower [mt]						
Pad Width		Number of pads				
[m]	[deg]	3	4	8	12	
0.7	20	21	23	134	360	
1.4	40	29	37	574	x	
2.1	60	37	91	x	x	
2.4	70	43	171	x	x	
2.8	80	55	361	x	x	

Buckling						
Clamping Capacity Wind Turbine Tower [kN]						
Pad Width		Number of pads				
[m]	[deg]	3	4	8	12	
0.7	20	11672	15929	20963	21002	
1.4	40	13008	16836	21050	x	
2.1	60	15055	18753	x	x	
2.4	70	15400	19552	x	x	
2.8	80	17510	20066	x	x	

Buckling						
Loading Capacity Wind Turbine Tower [mt]						
Pad Width		Number of pads				
[m]	[deg]	3	4	8	12	
0.7	20	117	159	210	210	
1.4	40	130	168	211	x	
2.1	60	151	188	x	x	
2.4	70	154	196	x	x	
2.8	80	175	201	x	x	

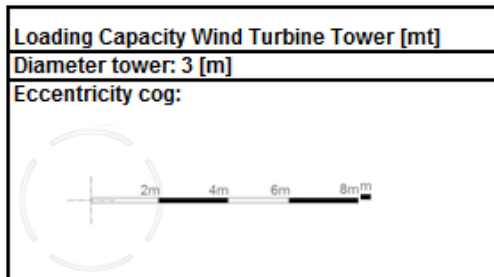
Yielding										
Clamping Capacity Wind Turbine Tower [kN]										
Pad Width		Number of pads								
[m]	[deg]	3	4	5	6	7	8	10	12	
0.7	20	2099	2285	3631	5806	9012	13429	23235	36000	

Yielding										
Loading Capacity Wind Turbine Tower [mt]										
Pad Width		Number of pads								
[m]	[deg]	3	4	5	6	7	8	10	12	
0.7	20	21	23	36	58	90	134	232	360	

Buckling										
Clamping Capacity Wind Turbine Tower [kN]										
Pad Width		Number of pads								
[m]	[deg]	3	4	5	6	7	8	10	12	
0.7	20	11672	15929	19155	20604	20937	20963	20716	21002	

Buckling										
Loading Capacity Wind Turbine Tower [mt]										
Pad Width		Number of pads								
[m]	[deg]	3	4	5	6	7	8	10	12	
0.7	20	117	159	192	206	209	210	207	210	

E.3. Diameter and Thickness (D=3m)



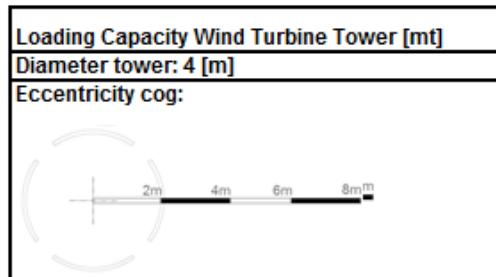
Thickness [mm]	Eccentricity [m]				
	0	2	4	6	8
14	96	89	71	41	23
16	134	127	109	84	67
18	179	173	155	128	111
20	233	227	208	173	155
22	296	289	253	218	201
24	368	361	299	264	246
26	449	410	345	310	293
28	541	457	392	358	340

Conditions		
Rubber Elasticity	1200	[Mpa]
Number of Pads	4	[-]
Width of pad	80	[deg]
Height of pad	3	[m]
Diameter Tower	3	[m]
Thickness Tower	14-28	[mm]
Eccentricity	0-8	[m]
Yield Strength	355	[Mpa]
Rubber Thicknes	110	[mm]
Rubber Elasticity	1200	[Mpa]
Friction Coefficie	0.15	[-]
sf yield	1.5	[-]
sf buckling	1.5	[-]
sf friction	1.5	[-]

Required Loading Capacity [mt]	
4MW Turbine	70
5MW Turbine	100
6MW Turbine	130
7MW Turbine	160

Legend	
Buckling failure	
Yielding failure	

E.4. Diameter and Thickness (D=4m)



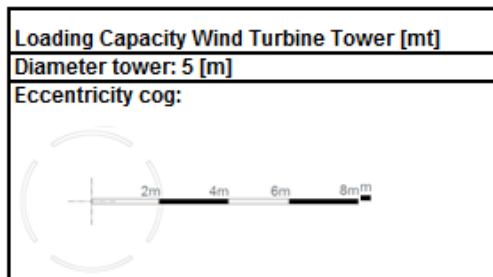
Thickness [mm]	Eccentricity [m]				
	0	2	4	6	8
16	116	109	91	67	50
18	155	149	131	109	90
20	202	195	177	153	135
22	256	250	231	197	179
24	319	312	276	241	224
26	389	383	321	287	269
28	468	432	368	333	315
30	557	479	414	380	362

Conditions		
Rubber Elasticity	1200	[Mpa]
Number of Pads	4	[-]
Width of pad	80	[deg]
Height of pad	3	[m]
Diameter Tower	4	[m]
Thickness Tower	16-30	[mm]
Eccentricity	0-8	[m]
Yield Strength	355	[Mpa]
Rubber Thickness	110	[mm]
Rubber Elasticity	1200	[Mpa]
Friction Coefficient	0.15	[-]
sf yield	1.5	[-]
sf buckling	1.5	[-]
sf friction	1.5	[-]

Required Loading Capacity [mt]	
4MW Turbine	70
5MW Turbine	100
6MW Turbine	130
7MW Turbine	160

Legend	
Buckling failure	
Yielding failure	

E.5. Diameter and Thickness (D=5m)




Thickness [mm]	Eccentricity [m]				
	0	2	4	6	8
18	139	132	114	91	74
20	181	174	156	133	115
22	229	223	205	175	158
24	285	278	253	219	201
26	348	342	298	263	246
28	419	408	343	308	291
30	498	454	389	354	337
32	585	500	436	401	384

Conditions		
Rubber Elasticity	1200	[Mpa]
Number of Pads	4	[-]
Width of pad	80	[deg]
Height of pad	3	[m]
Diameter Tower	5	[m]
Thickness Tower	18-32	[mm]
Eccentricity	0-8	[m]
Yield Strength	355	[Mpa]
Rubber Thicknes	110	[mm]
Rubber Elasticity	1200	[Mpa]
Friction Coefficie	0.15	[-]
sf yield	1.5	[-]
sf buckling	1.5	[-]
sf friction	1.5	[-]

Required Loading Capacity [mt]	
4MW Turbine	70
5MW Turbine	100
6MW Turbine	130
7MW Turbine	160

Legend	
Buckling failure	
Yielding failure	

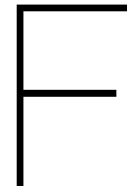
E.6. Diameter and Thickness (D=6m)

Loading Capacity Wind Turbine Tower [mt]					
Diameter tower: 6 [m]					
Eccentricity cog:					
					
Thickness [mm]	Eccentricity [m]				
	0	2	4	6	8
20	165	158	140	113	95
22	209	203	185	154	137
24	260	254	231	196	179
26	318	311	274	239	222
28	383	376	318	284	266
30	455	428	363	329	311
32	534	474	410	375	357
34	622	521	457	422	404

Conditions		
Rubber Elasticity	1200	[Mpa]
Number of Pads	4	[-]
Width of pad	80	[deg]
Height of pad	3	[m]
Diameter Tower	6	[m]
Thickness Tower	20-34	[mm]
Eccentricity	0-8	[m]
Yield Strength	355	[Mpa]
Rubber Thickness	110	[mm]
Rubber Elasticity	1200	[Mpa]
Friction Coefficient	0.15	[-]
sf yield	1.5	[-]
sf buckling	1.5	[-]
sf friction	1.5	[-]

Required Loading Capacity [mt]	
4MW Turbine	70
5MW Turbine	100
6MW Turbine	130
7MW Turbine	160

Legend	
Buckling failure	
Yielding failure	



Charts

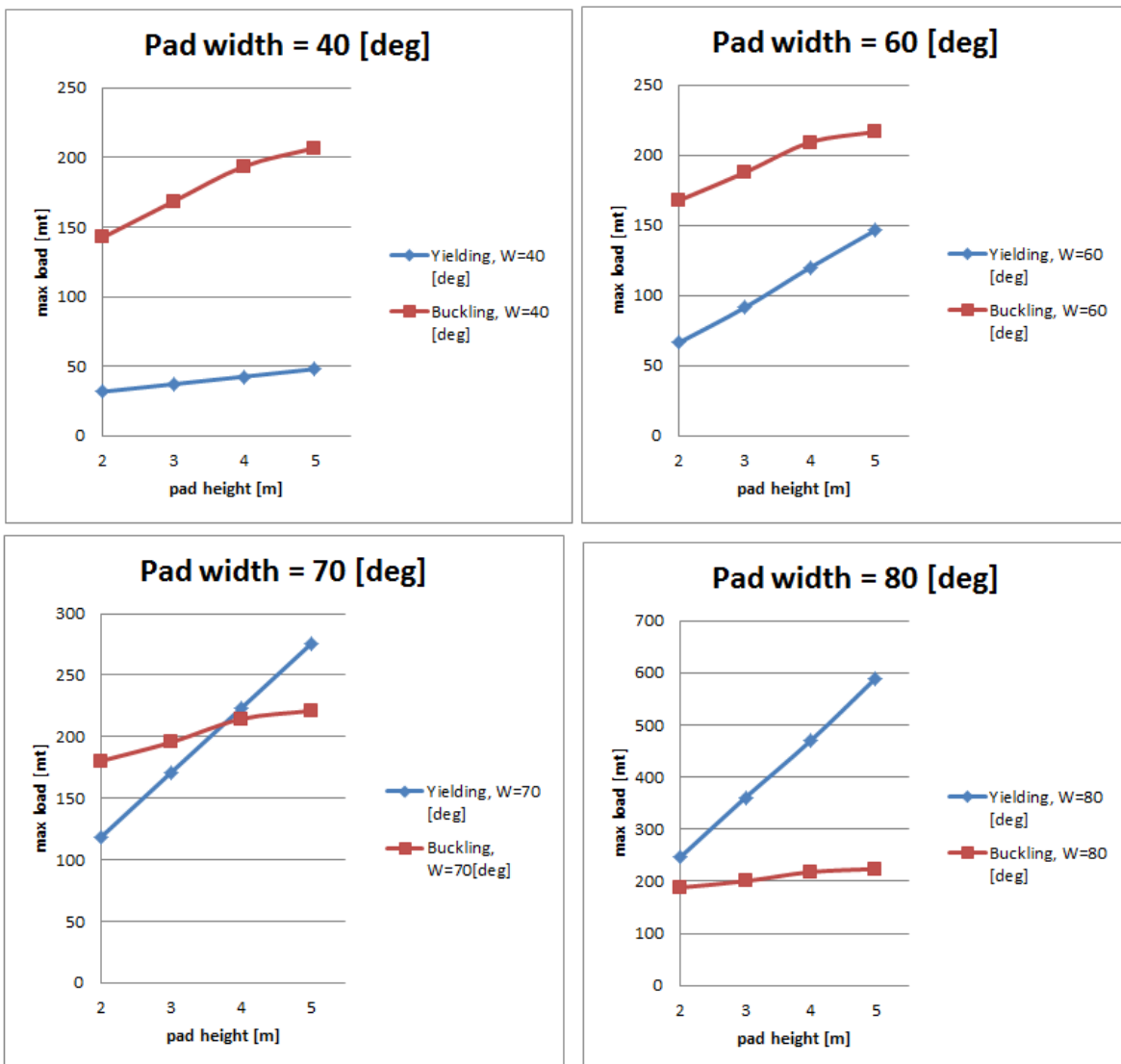


Figure E1: yielding and buckling load for a centred load (e=0)

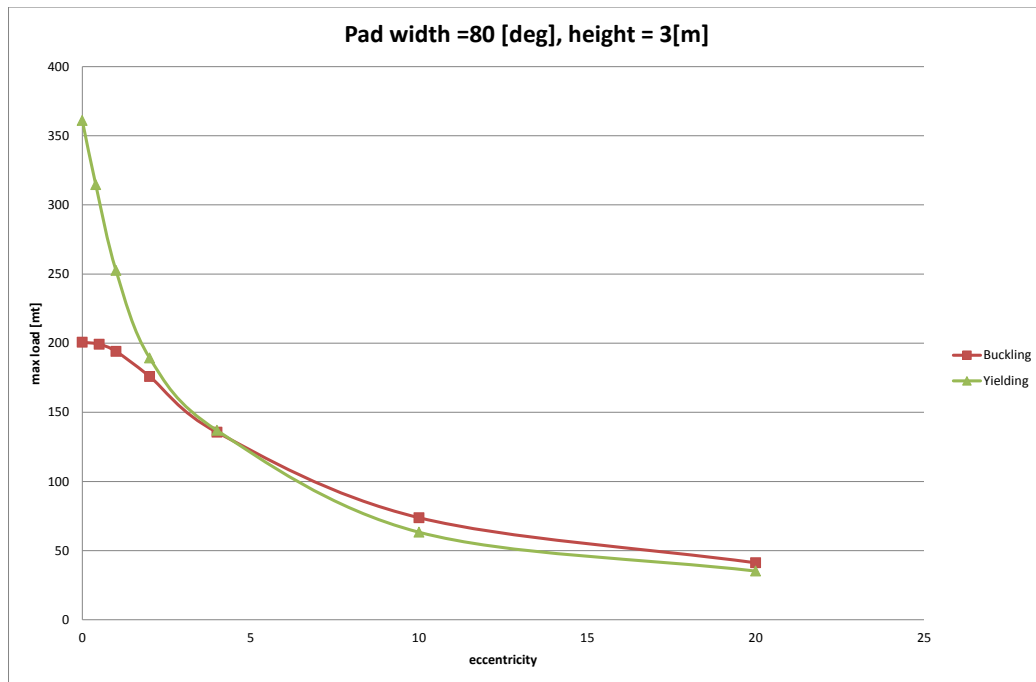


Figure E2: maximum load for yielding and buckling for increasing eccentricity

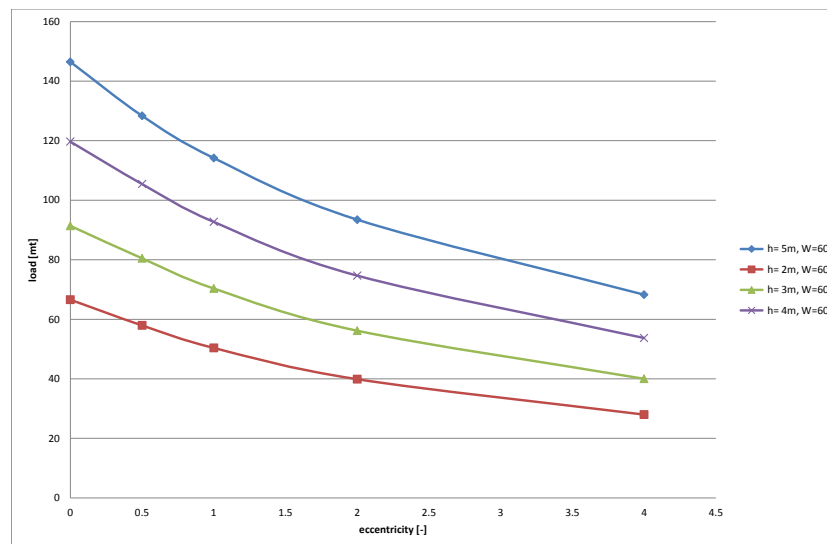


Figure E3: Maximum load for increasing eccentricity, W=60 deg

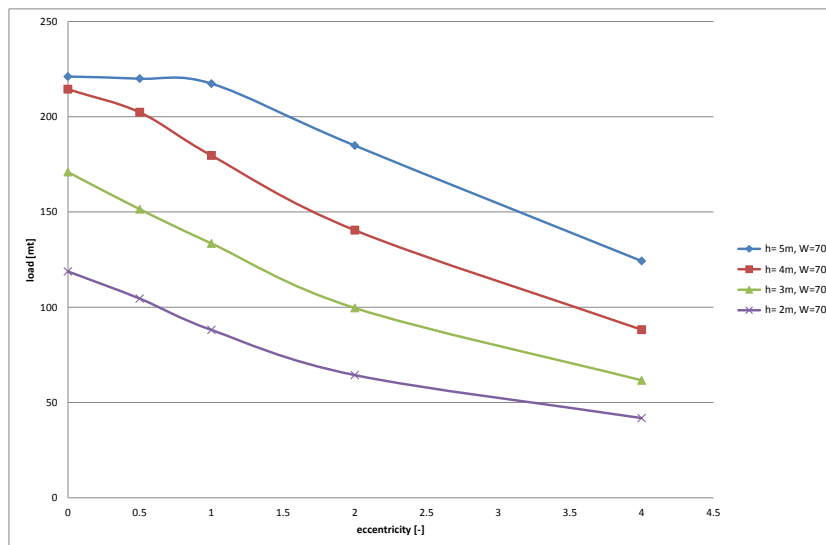


Figure E4: Maximum load for increasing eccentricity, W=70 deg

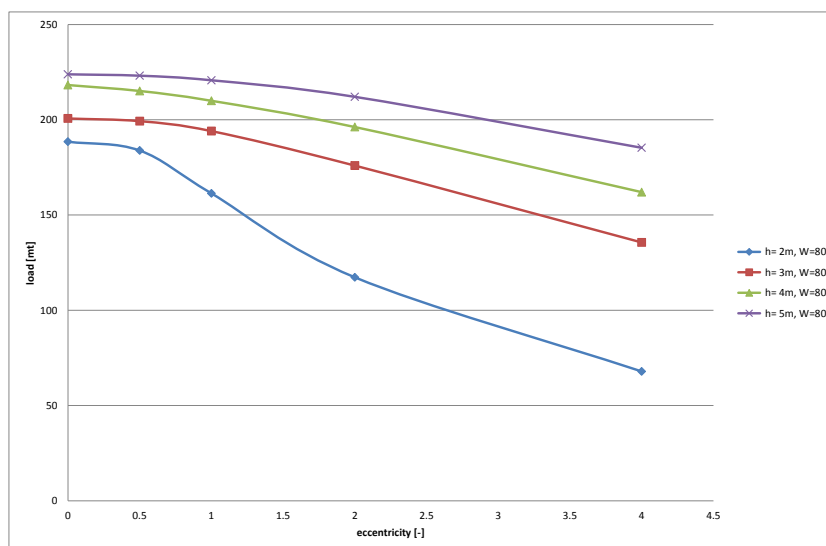
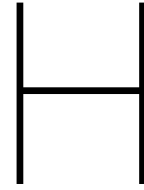


Figure E5: Maximum load for increasing eccentricity, W=80 deg



Eurocode correction for pipelength

An important difference between the used ANSYS model and the Eurocode is that the pressure is applied on a section of the tower (h in figure H.1) , and not on its complete length. To capture the effect of lengthening the tower section a pipe section is modelled in ANSYS, where the length of the section is increased (L in figure H.1) and the pressurized area is kept constant. The buckling pressure reduces substantially when the length of the tower section (L) is increased for a constant value of h. Convergence has been reached for $L > 7\text{m}$ and the correction factor can be determined:

$$\frac{P_{b,ANSYS}(L=7)}{P_{b,ANSYS}(L=H)} = f_{length} = 0.61 \quad (\text{H.1})$$

Where $P_{b,ANSYS}$ is the ANSYS buckling pressure and f_{length} is the correction factor which should be applied when using the eurocode pressure results and include the effects of lengthening the pipe (L).

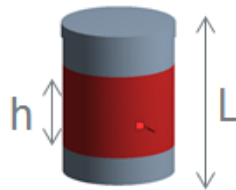


Figure H.1: Pipe section. Red area indicates the pressurized area

Bibliography

- [1] Nen-en-1993-1-6 (2007): Eurocode 3: Design of steel structures - part 1-6: Strength and stability of shell structures. *Part, 1*, 2007.
- [2] BO Almroth. Buckling of a cylindrical shell subjected to nonuniform external pressure. *Journal of Applied Mechanics*, 29(4):675–682, 1962.
- [3] BASF. Thermoplastic polyurethane elastomers, November 2017. URL http://www.polyurethanes.basf.de/pu/solutions/elastollan/en/function/conversions:/publish/content/group/Arbeitsgebiete_und_Produnkte/Thermoplastische_Spezialelastomere/Infomaterial/elastollan_material_uk.pdfm.
- [4] James Carroll, Alasdair McDonald, and David McMillan. Failure rate, repair time and unscheduled o&m cost analysis of offshore wind turbines. *Wind Energy*, 19(6):1107–1119, 2016.
- [5] DJ Cerda Salzmänn. Ampelmann: Development of the access system for offshore wind turbines. 2010.
- [6] Yalcin Dalgic, Iraklis Lazakis, and Osman Turan. Vessel charter rate estimation for offshore wind o&m activities. 2013.
- [7] Staffan Engström, Tomas Lyrner, Manouchehr Hassanzadeh, Thomas Stalin, and John Johansson. Tall towers for large wind turbines. *Report from Vindforsk project*, 342:50, 2010.
- [8] Stefan Faulstich, Berthold Hahn, and Peter J Tavner. Wind turbine downtime and its importance for offshore deployment. *Wind energy*, 14(3):327–337, 2011.
- [9] Huei-Huang Lee. *Finite Element Simulations with ANSYS Workbench 17*. SDC publications, 2017.
- [10] James F Manwell, Jon G McGowan, and Anthony L Rogers. *Wind energy explained: theory, design and application*. John Wiley & Sons, 2010.
- [11] Kyoto Protocol. United nations framework convention on climate change. *Kyoto Protocol, Kyoto*, 19, 1997.
- [12] C Rajakumar and CR Rogers. The lanczos algorithm applied to unsymmetric generalized eigenvalue problem. *International Journal for Numerical Methods in Engineering*, 32(5):1009–1026, 1991.
- [13] Lloyd's Register. code for lifting appliances in a marine environment. 1, 2013.
- [14] Arnaud Thiry, Philippe Rigo, Loïc Buldgen, Gregory Raboni, and Frederic Bair. Optimization of monopile offshore wind structures. *Marstruct*, 2011.
- [15] van den Bos. *Design With Finite Elements, WB3416-3*. Delft University of Technology.